AD-A076 209 NAVAL OCEAN SYSTEMS CENTER SAN DIEGO CA F/G 9/3
POWER ELECTRONICS TECHNOLOGY APPLICATIONS FOR FUTURE SSBNS - FY--ETC(U)
AUG 79 E KAMM
UNCLASSIFIED NOSC/TR-443 NL

| OF |
AD-
A076209

END
DATE
FILMED
11-79
DDC

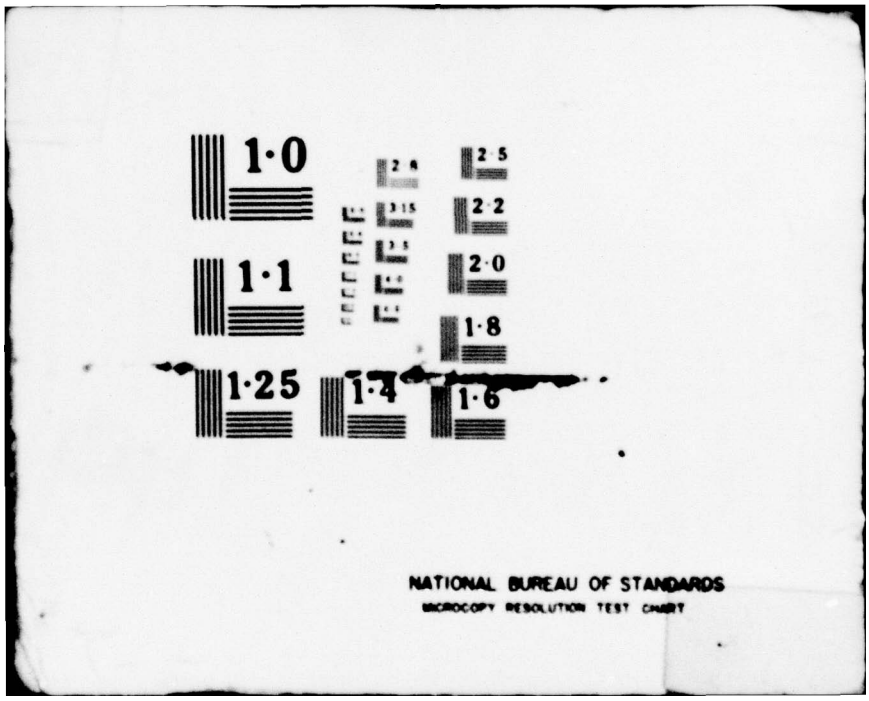
1·0
1·1
1·25
1·4
1·6
1·8
2·0
2·2
2·5
NATIONAL BUREAU OF STANDARDS
MICROCOPY RESOLUTION TEST CHART

NOSC

NOSC TR 443

NOSC TR 443

Technical Report 443

POWER ELECTRONICS TECHNOLOGY APPLICATIONS FOR FUTURE SSBNs - FY 78

Switching-mode power supply designs are compatible with sensitive SSBN circuits

E Kamm

1 August 1979

Final Report FY 78

Prepared for
Naval Sea Systems Command

NAVAL OCEAN SYSTEMS CENTER
SAN DIEGO, CALIFORNIA 92152

NAVAL OCEAN SYSTEMS CENTER, SAN DIEGO, CA 92152

AN ACTIVITY OF THE NAVAL MATERIAL COMMAND

SL GUILLE, CAPT, USN
Commander

HL BLOOD
Technical Director

ADMINISTRATIVE INFORMATION

This work was funded by NAVSEASYSCOM PMS-396 under work request N0002478WR8G204, program element 63588N, task 21577. This task is part of the Naval Sea Systems Command SSBN Subsystem Technology Program. The NAVSEA program coordinator for this task is Mr. Robert P. Draim, PMS 396-23. The work was performed by the author in the Power Electronics Branch, Code 9234, Advanced Applications Division, Electronics Engineering and Sciences Department, Engineering and Computer Sciences Directorate, Naval Ocean Systems Center, under project S0001-SB, task area S0001001, work unit EE07. The orientation of the work is on the impact of power electronics as used in electronic systems on the electrical subsystem.

This report is the second one for this project and covers work done in FY 78. The first report was published as NOSC TR 177 for work performed in FY 77.

Reviewed by
C. E. Holland, Head
Advanced Applications Division

Under authority of
C. D. Pierson, Jr., Head
Electronics Engineering and
Sciences Department

UNCLASSIFIED

SECURITY CLASSIFICATION OF THIS PAGE (When Data Entered)

REPORT DOCUMENTATION PAGE

READ INSTRUCTIONS BEFORE COMPLETING FORM

1. REPORT NUMBER: NOSC Technical Report 443

2. GOVT ACCESSION NO.

3. RECIPIENT'S CATALOG NUMBER

4. TITLE (and Subtitle): POWER ELECTRONICS TECHNOLOGY APPLICATIONS FOR FUTURE SSBNs – FY 78. Switching mode power supply designs are compatible with sensitive SSBN circuits

5. TYPE OF REPORT & PERIOD COVERED: Final Report, FY 78

6. PERFORMING ORG. REPORT NUMBER

7. AUTHOR(s): E. Kamm

8. CONTRACT OR GRANT NUMBER(s): S0001SB

9. PERFORMING ORGANIZATION NAME AND ADDRESS: Naval Ocean Systems Center, San Diego, CA 92152

10. PROGRAM ELEMENT, PROJECT, TASK AREA & WORK UNIT NUMBERS: 63588N – 21577; S0001-SB-S0001001-EE07

11. CONTROLLING OFFICE NAME AND ADDRESS: Naval Sea Systems Command, Washington, D.C.

12. REPORT DATE: 1 August 1979

13. NUMBER OF PAGES: 66

14. MONITORING AGENCY NAME & ADDRESS (if different from Controlling Office)

15. SECURITY CLASS. (of this report): Unclassified

15a. DECLASSIFICATION/DOWNGRADING SCHEDULE

16. DISTRIBUTION STATEMENT (of this Report)

Approved for public release; distribution unlimited.

17. DISTRIBUTION STATEMENT (of the abstract entered in Block 20, if different from Report)

18. SUPPLEMENTARY NOTES

19. KEY WORDS (Continue on reverse side if necessary and identify by block number)

20. ABSTRACT (Continue on reverse side if necessary and identify by block number)

The impact of switching-regulator noise on sensitive communication circuits is investigated. State-of-the-art switching-mode power supplies are shown to be compatible with sensitive receiver circuits including low-frequency receivers. Recent advances in component design and circuit design techniques that curtail or contain electromagnetic interference (EMI) in switching-mode converters are discussed. The frequency spectrums of the powerline-conducted EMI are analyzed for both ac and dc input designs. By using an optimally designed input filter, the emission caused by the switching action is shown to be less than expected new CE-03 limits for MIL-STD-461A. A major breakthrough in reducing EMI is a recently developed topology for switching-mode power supplies. → next page

DD FORM 1 JAN 73 1473 EDITION OF 1 NOV 65 IS OBSOLETE S/N 0102-LF-014-6601

UNCLASSIFIED

SECURITY CLASSIFICATION OF THIS PAGE (When Data Entered)

393 159

20. Continued.

Compared to dissipative power supplies, low voltage switching-mode power supplies occupy less volume, weigh less, cost less, and use less energy.

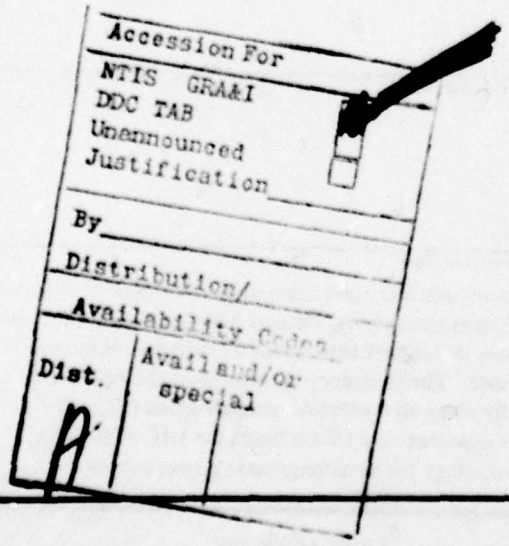

SUMMARY

OBJECTIVE

Overall Project

Identify and initiate development of power electronic technologies which will provide improved cost-effectiveness in the conversion and use of electrical energy by SSBN electronic systems, either through reduced cost, improved performance or both.

FY 78 Task

Determine the impact of switching-regulator noise on sensitive circuits, including low-frequency communication circuits. Initiate an assessment of the costs and benefits of powering a typical SSBN subsystem from a dc source and switching-mode power supplies.

RESULTS

1. Switching-mode power supplies can be compatible with sensitive receiver circuits.

2. Designs are available to curtail or contain electromagnetic interference (EMI) caused by the switching action.

3. State-of-the-art switching-mode power supplies can be designed to meet the expected new Navy CE-03 limits for MIL-STD-461A.

4. A major breakthrough in reducing EMI is a recently developed topology for switching-mode power supplies.

5. Ac-powered switching-mode converters decrease line rectification harmonics to the extent that they conserve power. Dc-powered switching-mode converters eliminate rectification harmonics.

6. Compared to dissipative power supplies, low-voltage switching-mode power supplies occupy less volume, weigh less, cost less, and use less energy.

RECOMMENDATIONS

The conclusion that switching-mode power supplies are compatible with sensitive circuits eliminates a roadblock to the candidate electrical power systems proposed in the first task (FY 77) for this project. Therefore, continuation of this study is recommended. For the next phase the following tasks are recommended:

1. Complete the cost/benefit assessment of using dc-input switching-mode power supplies in a typical SSBN subsystem.

2. Conceive a system design based on the candidate electric power configuration proposed in the first phase of this project, identifying components and subsystems that need major development.

CONTENTS

INTRODUCTION

The work described in this report is a follow-on effort to a previous task reported in NOSC TR 177 Revision A.[1] The previous task looked at the present SSBN approach for conversion and use of electrical energy by electronic systems. Problem areas were also examined. As alternatives, two basic candidate systems were proposed (figure 1). They are identical in that switching-mode power supplies accepting high-voltage dc (either 160- or 270-V dc) are used for all power conversion in the electronic systems. These switching-mode power supplies are smaller and lighter than conventional 400-Hz power supplies. Each configuration has a dc-link to provide continuity of power for critical loads.

The configurations differ in that configuration I (figure 1) is designed for an SSBN whose primary power source is dc, whereas configuration II is designed for an SSBN whose primary power source is ac. In addition to the switching regulator power supply's dc-to-dc conversion stage, configuration II requires an ac-to-dc power conversion stage, which can be part of either the electric power system (configuration IIA) or the electronic system (configuration IIB).

The proposed technology has a potentially high leverage for achieving the SSBN goals of lower life-cycle costs, improved performance, smaller size, and less weight. Potential advantages over the present approach also include lower initial cost, more efficient cooling, lower power consumption, higher reliability, and improved immunity to momentary power interruptions. The several power electronic technological advances that are central to this

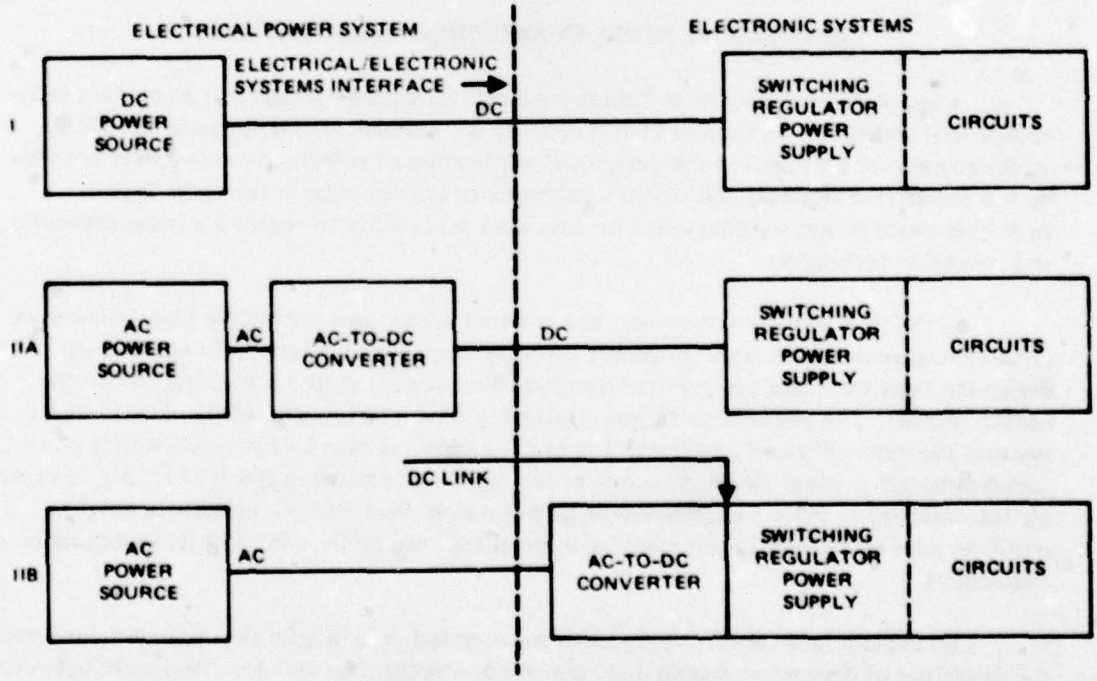

Figure 1. Candidate systems.

[1] NOSC TR 177 Revision A, "Power Electronics Technology Applications for Future SSBNs (U)," by J. Foutz and E. Kamm, 1 June 1978.

approach could be beneficial to future SSBNs whether or not alternatives I, IIA or IIB are selected.

The results of the preceding task led to the recommendation that a study of these proposed alternatives be continued to the point where sufficient information for a decision is available. The recommendations included key questions to be resolved and activities to be performed. Two of these key recommendations are the basis for the work described herein. They are as follows:

1. Determine the impact of switching-regulator noise on sensitive circuits, including low-frequency communication circuits.

2. Determine the cost and benefit to a typical electronic system that would be obtained by powering it from a dc source and switching-regulator power supply.

Because adverse findings in recommendation 1 could totally negate the approach, at least for some electronic systems, and because the results would be applicable to present programs, recommendation 1 was initially pursued.

For recommendation 2, work was initiated but not completed. Yet to be pursued is the following recommendation:

3. Conceive a system design, identifying components and subsystems that need major development.

ELECTRICAL NOISE IN SWITCHING-REGULATORS

A major shortcoming of switching-regulator technology is that it is a complex technology that appears to be simpler than it actually is. Because of this apparent simplicity, misjudgments are prevalent in the design and application of switching-mode power supplies by the uninitiated engineer. Nowhere was this more evident than in the early days of switching-mode power supplies when designs were made without regard for noise prevention and reduction techniques.

In the past few years, however, the inherent advantages (especially high efficiency) of switching-mode technology for power supplies have spurred advances in component design (to limit the noise sources) and design techniques (to curtail noise coupling to the outside world). The result is much less electromagnetic interference (EMI). Furthermore, because the more efficient power supplies may require less than half as much source power, a well-designed ac input switching-mode power supply can result in less EMI than a comparable less efficient ac input dissipative-type power supply (since all 60- or 400-Hz ac-to-dc rectifiers emit an EMI spectrum reaching beyond the commonly used 20-kHz switching-mode frequency).

To explain how power supply noise is generated, it is helpful first to comment upon the operation of dissipative and switching-mode power supplies and the differences between them. These differences and power supply functions in general are discussed in the following section.

POWER SUPPLY FUNCTIONS

A power supply is essentially a buffer circuit that matches a load to its power source. Ideally, for a load compatible with the source, the power supply function would be served merely by interconnecting wires. Usually the power supply function is more complex, requiring conversion and regulation of various electrical characteristics.

Power supply regulator circuits and power conversion circuits can be either dissipative or nondissipative. Dissipative regulators regulate by varying the amount of power they dissipate. For example, figure 2a depicts a series regulator in which the series pass element is indicated as a variable resistor, a functional representation. The worst wattage conditions occur at high-input line voltage and low-output voltage. The undelivered power is converted to heat and removed by a cooling system. One type of nondissipative regulator commonly used is a switching regulator that regulates by varying the amount of power it lets through during a switching cycle. This is done by varying the relative ON time of the switch (figure 2B). Power is not absorbed. Power "losses" (conversion to wasted heat) are caused by less than ideal components. Switching is usually in the 10- to 100-kHz range, although higher frequencies are starting to be used. This technology can provide power conversion equipment that is independent of powerline frequency.

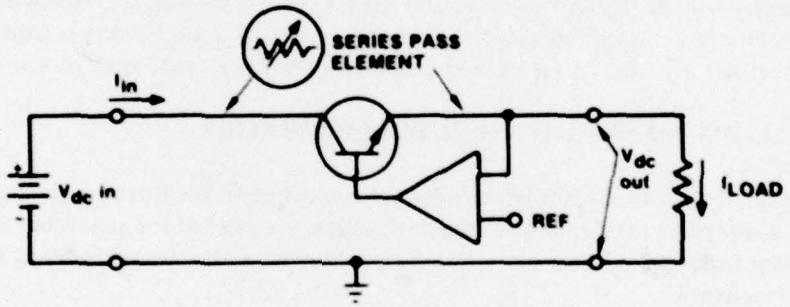

(a) SERIES PASS REGULATOR

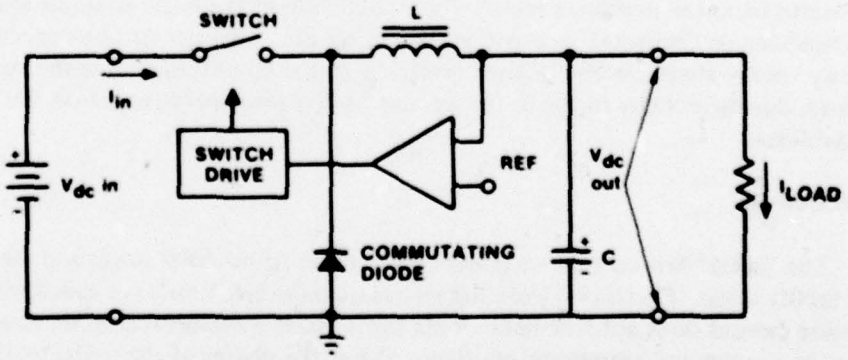

(b) SWITCHING MODE REGULATOR

Figure 2. Simplified diagrams of typical series pass and switching mode regulators.

Regardless of whether a dissipative or switching-mode regulator is used, conversion from ac to dc will generate EMI due to the rectification process. If rectification is not required as in a dc electrical power system, then this source of predominantly low frequency EMI does not exist. Switching-mode power supplies match the requirements of dc power systems because isolation can readily be achieved with a transformer at the switching frequency whereas a simple isolation solution does not exist if dissipative power supplies are used in dc systems. Although there are overlapping frequencies, switching regulators, due to the switching action, are potential generators of EMI noise at higher frequencies than the noise produced by rectification.

The type of switching-mode power supply proposed in this project is called an off-line switching-mode power supply. Off-line connotes that ac power is immediately rectified to dc and power conversion is performed at frequencies well above line frequency. There are two types of off-line switching-mode power supplies – duty-cycle converters and resonant converters. The duty-cycle type regulates by varying the ratio of switch ON time to OFF time. It is the one usually referred to as a switching-mode regulator and is the one discussed in the preceding paragraph as a potential generator of EMI. The resonant type in one version regulates by varying the repetition rate of resonant pulses. Another version regulates by constructing two phase-shifted sine waves from a series of resonant pulses and vectorially adding them in an isolation transformer. A salient feature of both versions of resonant converters is minimal high-frequency EMI due to the filtering of the resonant circuit. Their features make them attractive for the higher power and/or higher voltage converters. Since off-line switching-mode power supplies using duty-cycle modulation are the worst case insofar as EMI is concerned, the rest of this report deals with the duty-cycle type power supply.

RECTIFICATION NOISE IN AC-TO-DC POWER SUPPLIES

Figure 3 depicts the bridge rectifier commonly used for three-phase inputs. The transformer, required for dissipative power-supplies, is optional for switching-mode power supplies since isolation is more cost-effectively achieved with a transformer at the higher switching frequency.

The rectification process yields two sources of harmonic emission spectra which are conducted on the input power lines (distorting the sinusoidal input). The first and major source stems from the nonlinear rectification distortion of the basic ac sinusoidal function. A step function or "staircase" current waveform results. The second noise spectrum is caused by energy stored, in the leakage reactance of the circuit, including the transformer secondary, during rectifier turn-off. As a result, spikes are superimposed on the basic staircase waveform.

Basic Waveform

The "ideal" line current waveform is shown in figure 4 for single and three-phase bridge rectification. Rectifiers operating into large inductive filters are called ideal because the dc-line current does not fluctuate. Both three-phase waveforms contain identical harmonics (in number and amplitude, see figure 5) but the phases of the individual harmonics do not correspond, which explains the differences in the waveforms. It should be noted that the spectrum shown in figure 5 and discussed here may be modified in some circuits by harmonic currents generated from the magnetizing current of iron-core transformers, and by

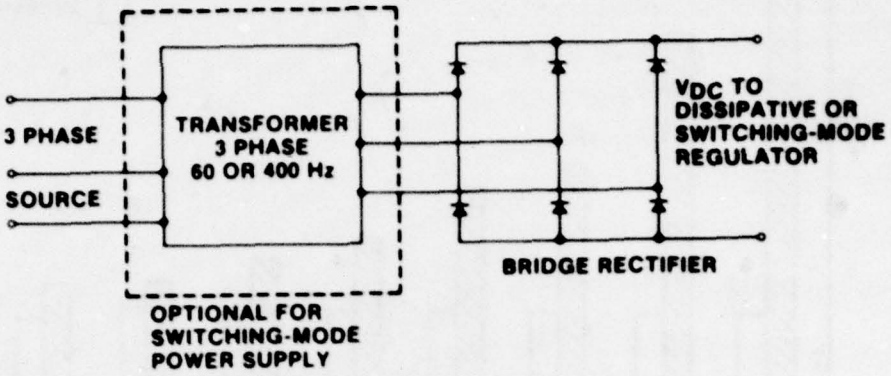

Figure 3. Three-phase bridge rectification.

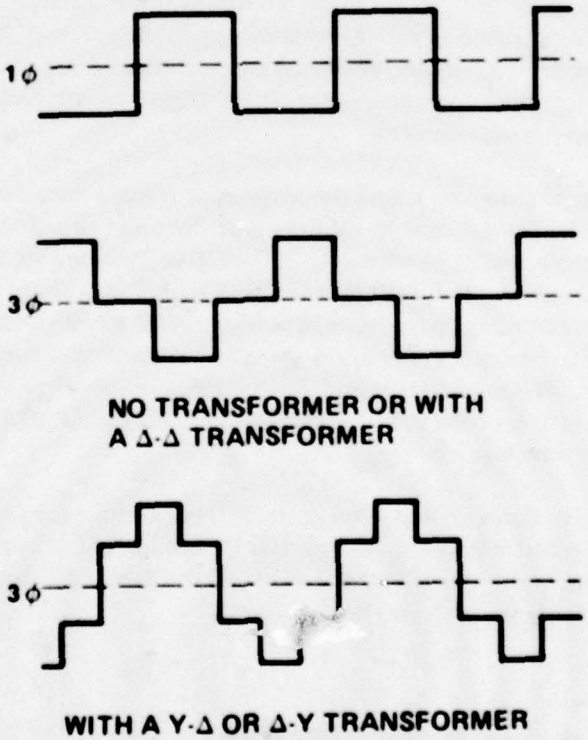

Figure 4. "Ideal" line current waveform.

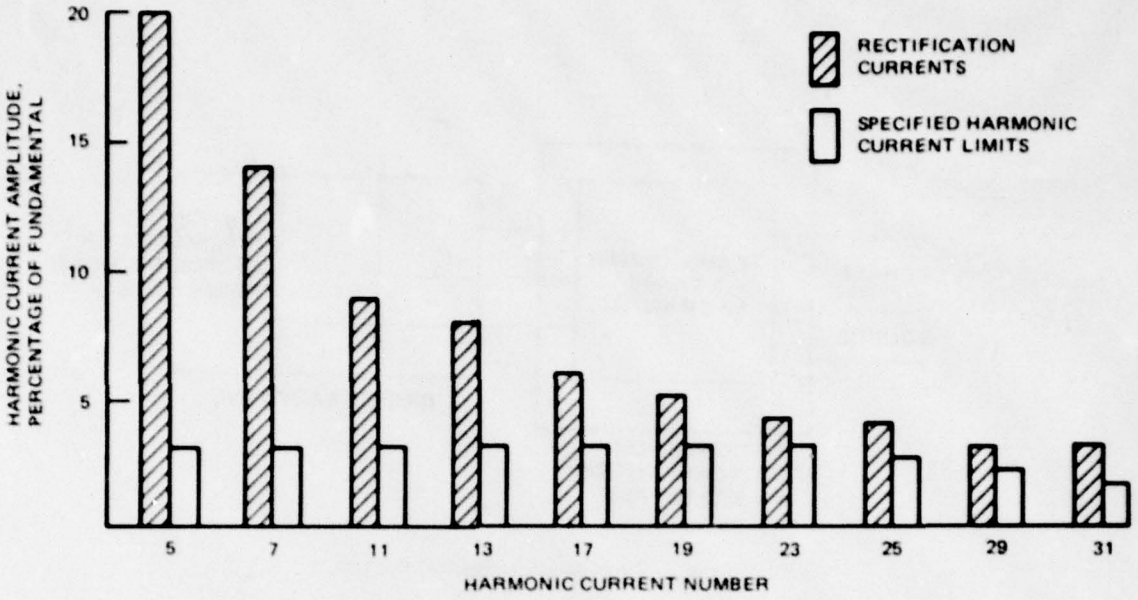

Figure 5. Harmonic currents caused by 6-pulse bridge rectification.

"abnormal harmonics" due to voltage imbalance in three-phase systems and other effects.[2] A more radical change in the "ideal" spectrum occurs if the input filters are capacitive which causes the lower-order harmonics to increase in magnitude and the higher-order ones to decrease in magnitude.[3] Harmonic problems are exacerbated because lower-order harmonics are more difficult to filter. Inductive input filters, therefore, are preferred to capacitive input filters for Navy power supplies.

Even for large inductive filters the waveshape is not a zero rise time step but more like a trapezoid. The typical current risetime is of the order of one or two microseconds without a transformer, and approximately 200 microseconds with a transformer (the leakage inductance slows down the rise (fall) times). Both with and without a transformer, the basic current waveforms can be approximated by a trapezoidal waveform. The Fourier transformation from time to frequency domain is given in Appendix A wherein the rationale for representing the waveform as a trapezoid is also given. Although the individual frequency spectra are different, the envelopes of maximum amplitudes are identical for both the real and approximated waveforms.

The curves in figures 6 and 7 are plots of this envelope for full-wave bridge rectifiers with and without transformers for 60- and 400-Hz fundamentals normalized to one ampere. Note that for a slower rise time (with transformer) the 40-dB-per-decade drop-off starts at a lower frequency, $1/\pi t_r$ (where t_r is the rise time).

---

[2]NOSC TD 107, "Reduction of Shipboard 400-Hz Power Requirements," by E. Kamm and J. Foutz, 16 May 1977.

[3]University of Pennsylvania Technical Report 77-3, "Modeling of Harmonics on Power Systems," by R. M. Showers and C. P. Kocher, May 1977 (prepared for NAVSEA 0271-ADB018735).

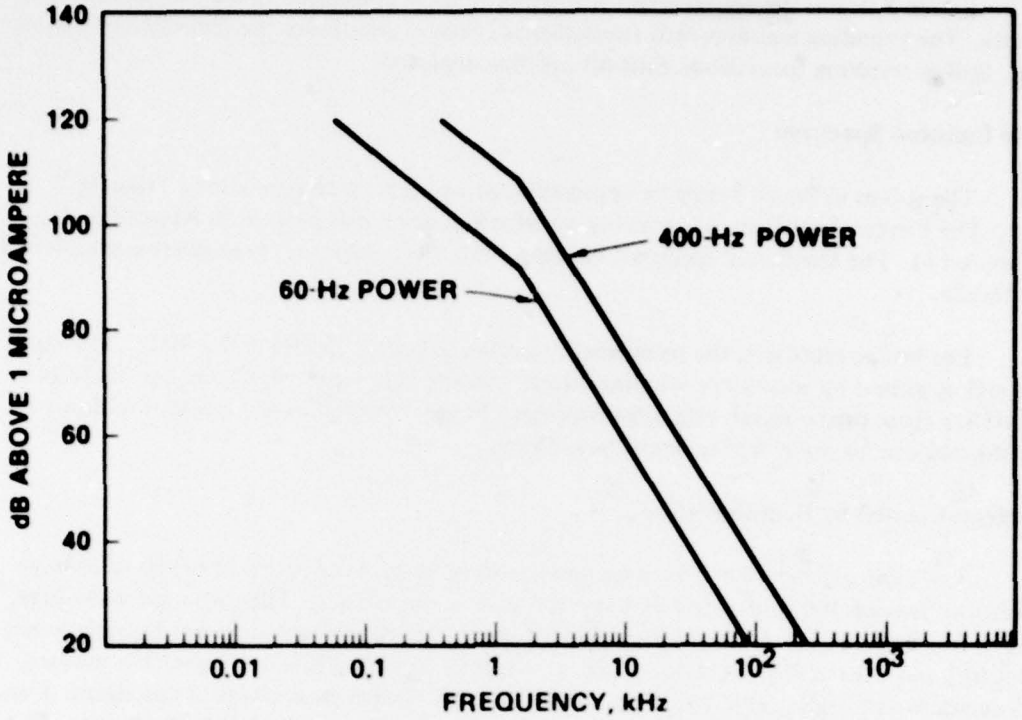

Figure 6. Normalized conducted frequency spectrum of transformer-rectifier power supply.

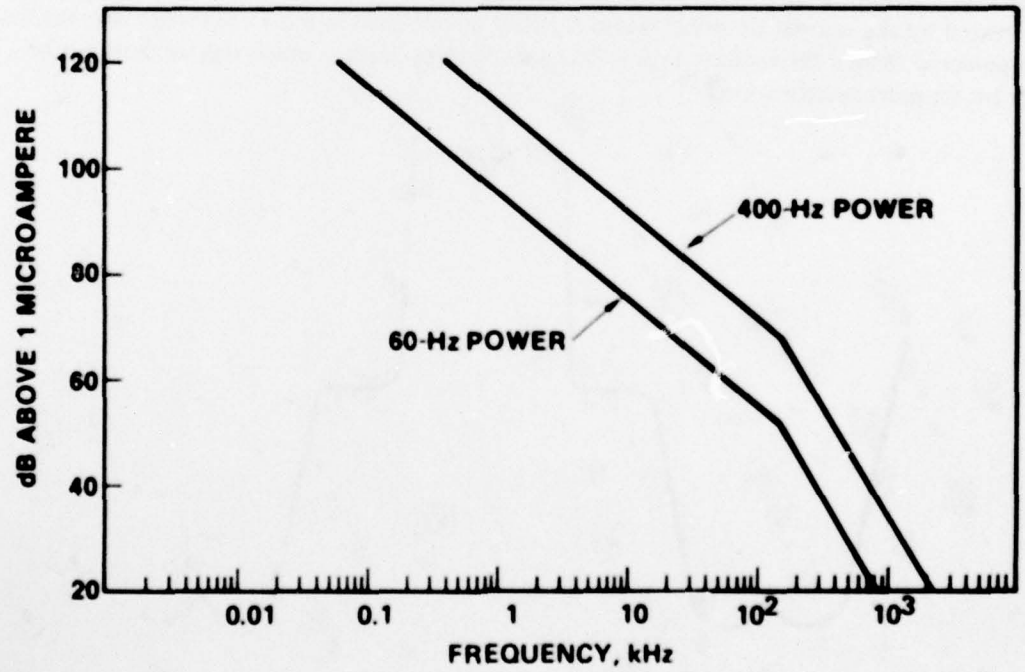

Figure 7. Normalized conducted frequency spectrum of a full-wave bridge rectifier without transformer.

Figure 8 shows the actual waveform likely to be encountered in transformer-rectifier circuits. The rounding and non-zero rise/fall-times effects arise from the transformer inductance. Spikes resulting from diode turn-off are also depicted.

Spike Emission Spectrum

The spikes in figure 8 may be approximated by either a trapezoid or a "ringing" spike. The Fourier transform of a ringing waveform is given and plotted in Appendix A (figure A-11). The frequency spectrum envelope exhibits a peak and then decreases at 40 dB per decade.

For bridge rectifiers, the peak usually occurs between 50 kHz and 2 MHz. The current spikes caused by secondary winding energy storage being interrupted by the diode turning off are more pronounced with a transformer. Some "spiking" is still present without a transformer due to input wiring resonance effects.

Problems Created by Rectifier Noise

The main effect of harmonic currents in an ac system is distortion of the ac voltage waveform through the source and distribution system impedance. The distorted waveform, in turn, can cause problems in poorly designed electronic equipment, increased power losses in motors and other magnetic devices, reduced torque in high-efficiency induction motors, and excitation of undesirable vibration modes through electrical-mechanical couplings. Furthermore, a distorted waveform can act as a driving source for submarine hull currents. For these reasons, recently revised specifications place a 3-percent limit on the amplitude of any harmonic current. Figure 5 shows the relationship of the 3-percent limit to the harmonics generated by the normal six-pulse bridge rectifier circuit used in most electronic systems that are powered from a three-phase source (the specification limit is much tighter than can be met by six-pulse rectification).

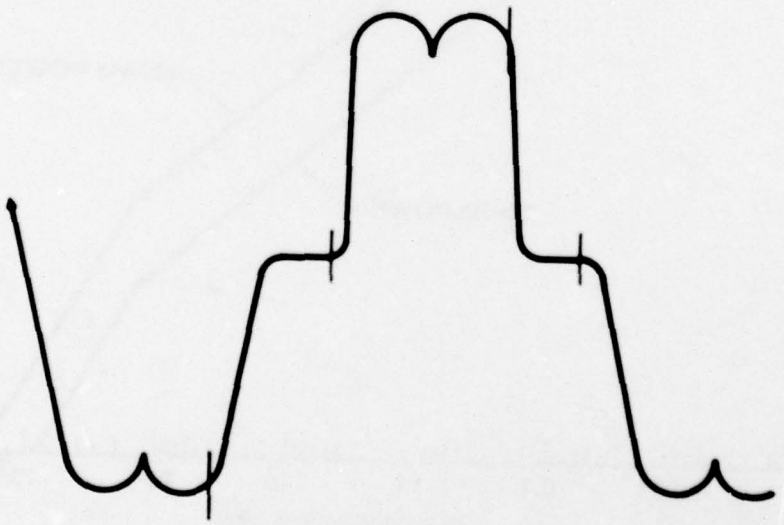

Figure 8. Typical per phase current waveform of a 3-phase transformer-rectifier power supply.

The approaches used to reduce harmonics include 12- or 24-pulse rectification, harmonic traps, and low-pass filters. New improved approaches[4,5,6] are being worked on but have not yet been completely developed. They all take advantage of switching-mode technology.

Reference 4 proposes an ac-to-dc converter in which the rectified waveform is chopped and pulse-width-controlled to improve the line current waveform. Reference 5 describes a switching-mode system in which a noisy 60-Hz line is fed into a bandpass filter and emerges clean. This system removes voltage surges as well as harmonics. In both references the statement is made that the high chopper frequency ($\simeq$ 20 kHz) is easily removed by a low-pass filter compared to more difficult filtering required at low rectification frequencies.

A technique developed under Army sponsorship (reference 6) may be the most promising approach. It uses three parallel off-line switching-mode power supplies whose outputs are tied together to form a single dc output. The inputs are derived from three separate diode bridges that appear as balanced single phase loads to the power system. The input impedance of the off-line converters are made to appear resistive. Since single-phase rectification into a resistive load produces no harmonics, the method reduces harmonics to the 3-percent limit requirement with no filtering. The need for three small switching mode converters in place of one large one may appear to be a drawback; however, in many applications it may be an advantage. It provides a method of increasing power output that might otherwise be limited by components and can be used for increasing power supply reliability by redundancy. The failure of one power supply reduces the output capability by one third and unbalances the load presented to the power system. Since any single power supply is a small load compared to the total power system capacity, this has no system effect.

Impact of Candidate Subsystems on ac-to-dc Rectifier Noise

The proposed subsystem I (figure 1) eliminates the harmonic current problem altogether. Subsystem II shifts the harmonic problem out of each individual electronic system into one or a limited number of points in the power system. The harmonic magnitudes, however, will be decreased because the more efficient switching regulator power supply will draw less current and correspondingly lower harmonic amplitudes. If the low-frequency transformer is eliminated, then the basic harmonic envelope spectrum will not decrease as rapidly (figures 6 and 7) but high-frequency "spiking" harmonics will decrease because the magnetics amplify the spikes.

SWITCHING-FREQUENCY NOISE IN CANDIDATE SYSTEMS

All three proposed candidate systems (figure 1) are potential generators of switching-frequency fundamental and harmonics as a result of the switching action. This source of

[4]Kataoka, T., Mizumadii, K. and Miyairi, S., "A Pulse Width Controlled AC to DC Converter to Improve Power Factor and Waveform of AC Line Current," paper presented to the IEEE International Semiconductor Power Converter Conference, Orlando, Florida, 28 March 1977.

[5]Nienhaus, H. A., Bowers, J. C. and Brooks, J. L., "An Active Power Bandpass Filter, Solid-State Power Conversion," Vol 4, No. 4, pp. 14-23, July/August 1978.

[6]Delco Electronics Report R78-38, "15KW General Purpose Power Conditioner (frequency changer) Final Report AC-DC Section," Contract DAAK70-77-C-0035, April 1978.

noise is not present in dissipative power supplies although, as previously discussed, comparable noise frequencies are present from ac-to-dc rectification. The main noise sources of switching frequency and its harmonics are the switching transistor (or thyristor) and the commutating diode. Figure 9 shows a simplified buck-switching regulator using a power transistor as the switching element. Figure 10 depicts the transistor current waveform for the buck-switching regulator in the continuous mode. The basic waveforms are given in Appendix B for the buck and other types of switching regulators. The buck waveform was selected because it represents the maximum line-conducted EMI compared to other types of switching regulators (the boost results in less EMI and the buck-boost results in the same EMI as the buck). Superimposed on the basic transistor waveform is a turn-on spike caused by the diode recovery current (also shown in figure 10).

Basic Waveform

The basic switching waveform (without considering the diode action) is shown in figure 11 where T is the period for one cycle (50 μsec for 20 kHz). A rise time, t_r, for the transistor is also shown (for simplicity it was not shown in figure 10). Rise times will vary with different transistors. A fast rise time will decrease heat losses (more efficient) but will result in more potential EMI. Typical rise/fall times associated with the switches are of the order of 100 nsec. As shown in Appendix B, the waveform (figure 11) represents operation in the continuous mode for $d > 0$. Operation in the discontinuous mode would be represented by $d = 0$.

Fourier Transform of Basic Waveform. For both continuous and discontinuous operation, the basic waveform can be modeled as a trapezoid to obtain the Fourier transform. As explained in Appendix A, the low frequency interference levels are identical for many pulse shapes. Above a frequency of approximately 1/(pulse width), the frequency level is determined by the rise and fall times of the pulse.

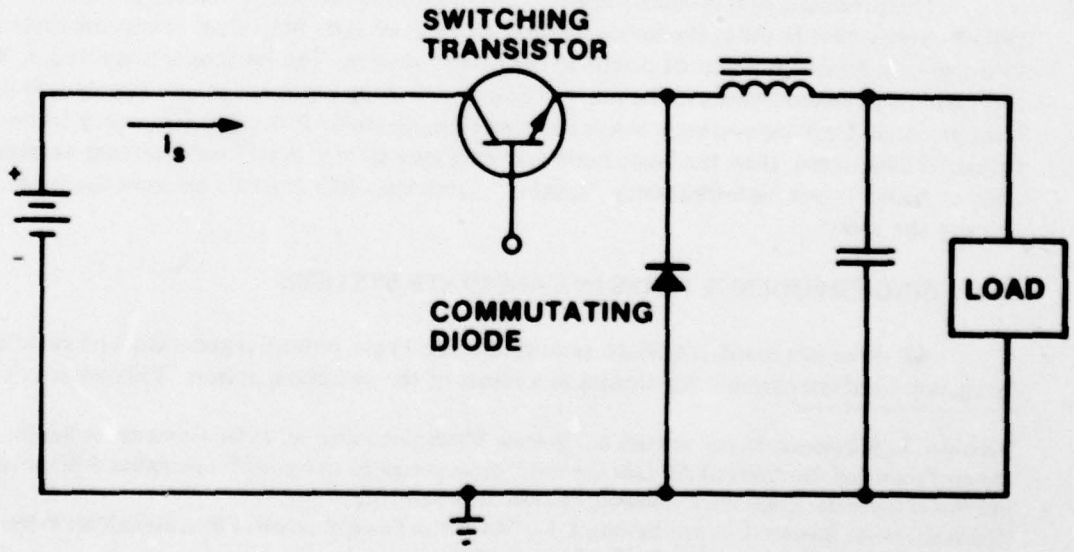

Figure 9. Noise sources for dc-input switching regulators.

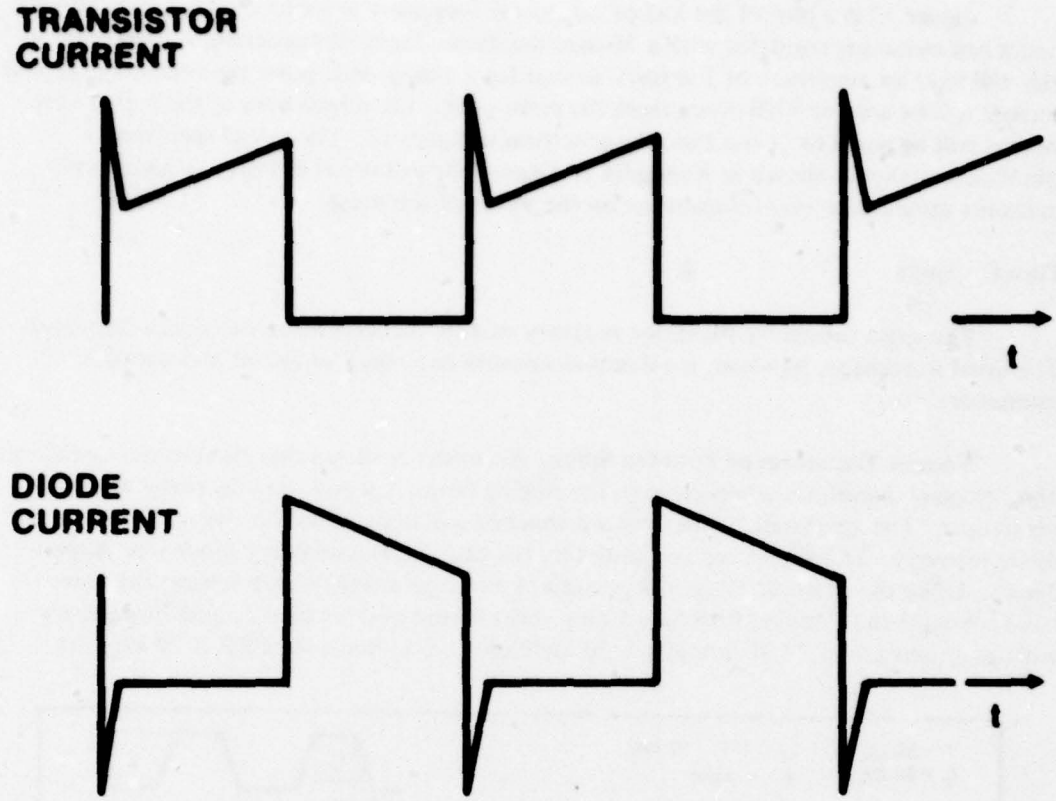

Figure 10. Switching transistor and commutating diode currents for simplified buck-switching regulator.

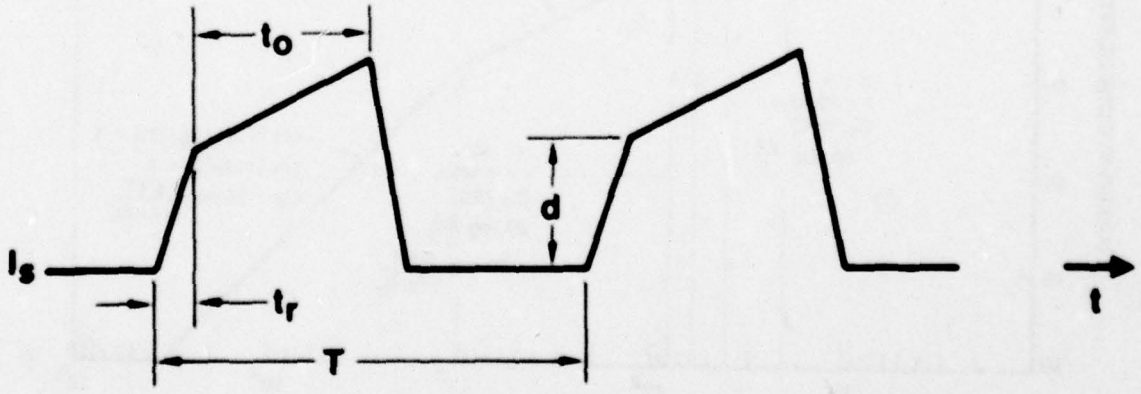

Figure 11. Switching-current basic waveform (without diode recovery spike).

Figure 12 is a plot of the loci of maximum frequency amplitudes (C_N) for a 20-kHz frequency switching regulator with a 30-nsec rise time. The first harmonic, a 20-kHz sinusoid, will have an amplitude of 2 amps/π so that for a 1-amp peak pulse the fundamental peak current is 0.64 amp or 4 dB down from the pulse peak. The amplitudes of the higher harmonics will be equal to or less than the spectrum in figure 12. The actual spectrum, a (sin x)/x function as shown in Appendix A, figure A-5, will result in lower or zero amplitudes for some frequencies, depending on the width of the pulse.

Turn-On Spike

The spike caused by the diode recovery current can also be modeled as a trapezoid. The usual waveshape, however, is a damped sinusoid as a result of circuit and parasitic resonances.

Fourier Transform of Turn-On Spike. Appendix A shows that the Fourier transform of a "ringing" waveform peaks close to the ringing frequency and then decreases at 40 dB per decade. The amplitude of the damped sinusoid will depend on the characteristics of the diode recovery. This effect can be limited by the use of a fast recovery diode (see Appendix F). Using the example given in Appendix A but converting to narrowband (narrowband = broadband + 20 log PRR*), a 1-amp spike would peak at the "ringing" frequency with an amplitude of 72 dB/μA/kHz + 20 log PRR (kHz). Since the PRR is 20 kHz, the

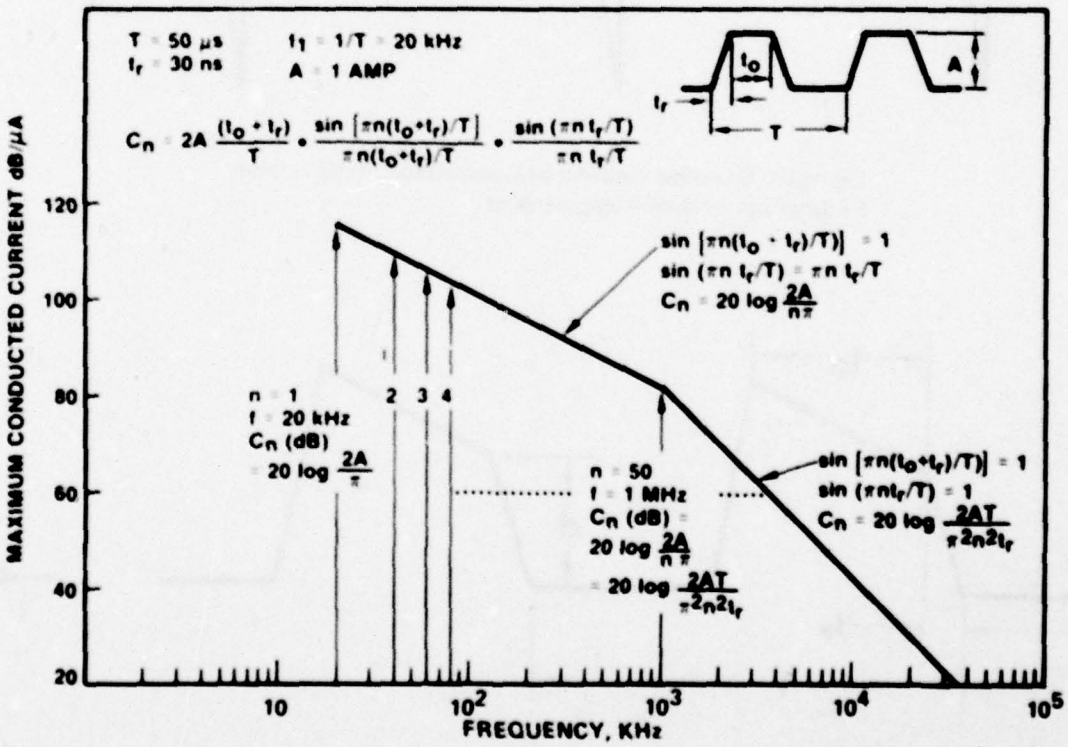

Figure 12. Switching regulator basic waveform harmonic spectrum.

*Pulse Repetition Rate

amplitude becomes 72 dB + 26 dB = 98 dB/μA. The individual frequencies would start at the PRR with a lower amplitude. Figure 13 is a plot of the loci of maximum frequencies for a 1-amp "ringing" spike with a peak at 3 MHz and attenuation, α, of 1.153×10^5 nepers.

Resultant Conducted Noise Spectrum

Figure 14 is the noise spectrum plot combined from both the basic waveform and the turn-on spike. The resultant envelope is shown extended at the low frequency end to account for subharmonic frequencies caused by potential imbalances when multiple switching transistors are used in the regulator design (push-pull or bridge operation). This resultant noise spectrum assumes no EMI filter.

The lower curves in figure 15 show the theoretical, typical spectrum attainable using a two-section LC filter. EMI filters can be designed as a single-section low-pass filter or by cascading several single-section filters to obtain more attenuation. Dr. Yu[7] demonstrates that a two-stage filter results in a lighter optimum weight than a single-stage filter when both are designed to meet identical peaking, attenuation, and efficiency requirements. This two-stage filter is further discussed in a previous paper by Yu and Biess[8] where component types are recommended based on the filter's operation (see Appendix C). Methodologies and computer programs for optimum power processing circuits (such as these filters) used in switching-regulator power supplies have been developed for the NASA "Modeling and Analysis of Power Processing Systems" (MAPPS) program. The two-stage filter spectra in figure 14 are developed in Appendix C by analysis techniques demonstrated by Dr. Middlebrook,[9] who also prefers a two-section LC filter, but for a different reason. Dr. Middlebrook gives design criteria for switching regulator's input filter to prevent instability. Limits are placed on the filter's output impedance peak magnitude, $|Z_S|$. Greater flexibility is achieved with a two-section filter, since a higher $|Z_S|$ peak can be allowed at the lower of the two resonant frequencies.

The attenuation curves shown in Appendix C assume ideal components (L, C and R) which are frequency-invariant. This is, of course, not true. In particular for the capacitor, capacitance varies with frequency. In addition, a capacitor has not only an equivalent series resistance (ESR) but also an equivalent series inductance (ESL). See Appendix C (page 50) for a more detailed discussion about recommended filter capacitors for switching-mode power supplies.

Figure 15 depicts plots of the powerline noise current without and with a two-stage input filter (designed for 54-dB attenuation at 20 kHz). The dotted line shows the theoretical attenuation slope if the filter capacitance values were invariant with frequency and negligible ESR and ESL existed. For the frequency region shown, the unfiltered noise declines at a 20-dB slope and the filtering at a 60-dB slope so the maximum attainable slope is 80 dB

---

[7]Yu, Y., et al. (TRW Defense & Space Systems), "Formulation of a Methodology for Power Circuit Design Optimization," paper presented at IEEE Power Electronics Specialists Conference, Cleveland, OH, June 1976.

[8]Yu, Y. and Biess, J. J., "Some Design Aspects Concerning Input Filters for DC-DC Converters," paper presented at the IEEE Power Conditioning Specialists Conference, Pasadena, CA, April 1971.

[9]Middlebrook, R. D., "Input Filter Considerations in Design and Application of Switching Regulators," paper presented at the IEEE Industry Applications Society Annual Meeting, Chicago, IL, October 1976.

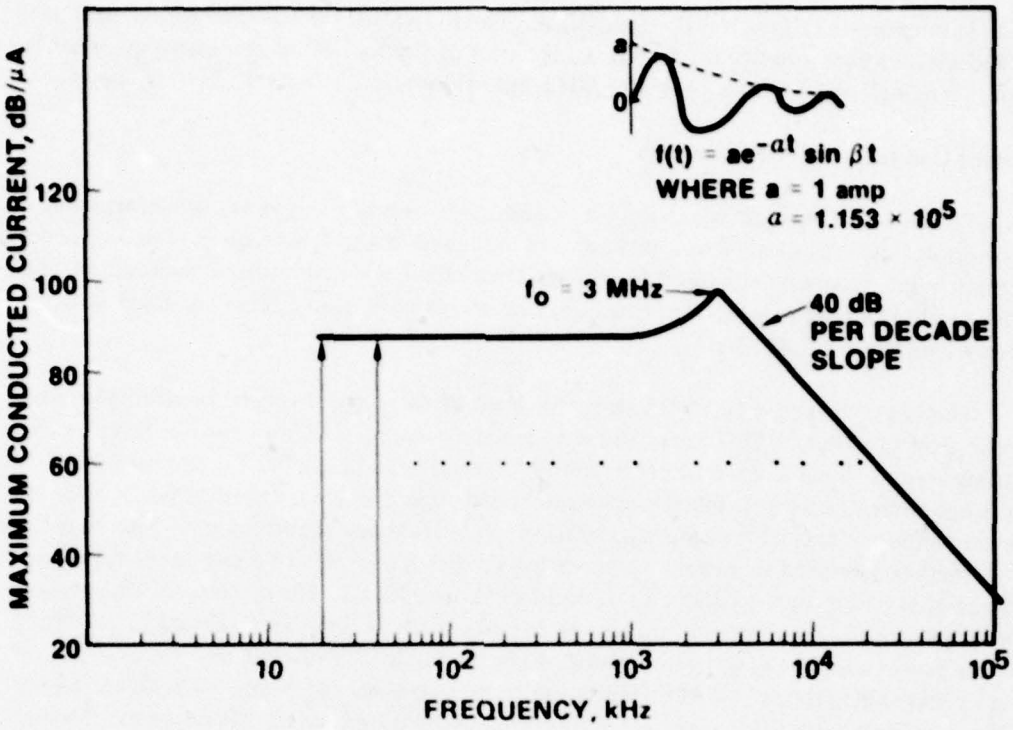

Figure 13. An example of switching regulator spike "ringing" spectrum (from diode recovery).

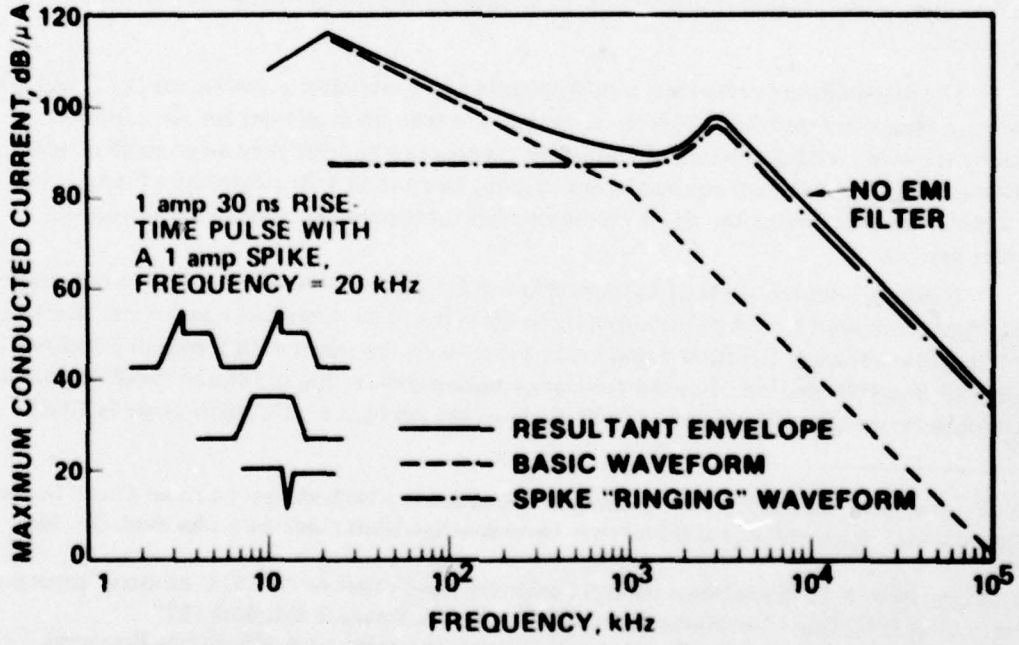

Figure 14. Switching regulator input current spectrum (no filter).

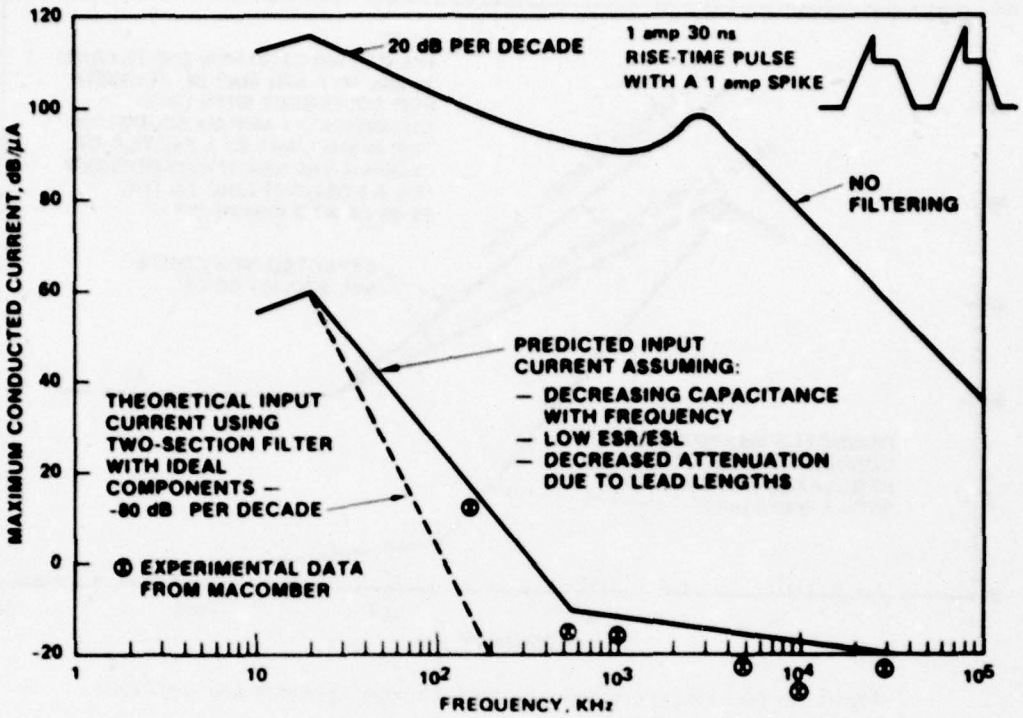

Figure 15. Switching regulator input current without and with filter (two stage).

per decade. A more realistic curve is represented by a solid line which assumes (a) capacitors are chosen to have the specified values at the switching frequency (but decrease with increasing frequency); (b) ESR and ESL values are low, with ESL between 1 and 15 nH; and (c) lead lengths cause about 10 dB less attenuation at 1 MHz. Macomber[10] recommends particular capacitors and gives experimental data which are noted in figure 15.

Figure 16 compares the predicted (realistic) noise current with the expected new Navy CE-03 limits* for MIL-STD 461A. The predicted envelope (a worst-case prediction) is below the expected new limits for load currents of 1 amp and below. For load currents greater than 1 amp and up to 2 MHz, the new limits are relaxed in proportion to the increased current and, therefore, the predicted noise levels remain below the relaxed limits up to 2 MHz. However, limits are exceeded above 2 MHz for load currents greater than 45 amps (153 dBμ A). High power loads of such magnitude, however, often use a resonant-type switching converter which generate minimal high frequency EMI and a high frequency EMI filter can be added to the basic two-section filter.

---

[10]Macomber, L. L., "Switching Regulator Capacitor Technology: Optimizing Ripple and EMI Suppression Performance," paper presented at POWERCON 5 in San Francisco, CA, 6 May 1978.

*FONECON between W. Jackson, NAVELEX 51024, and E. Kamm, NOSC 9234, on 29 November 1978. These limits are being used now for new equipment and they are being incorporated into MIL-STD-461E.

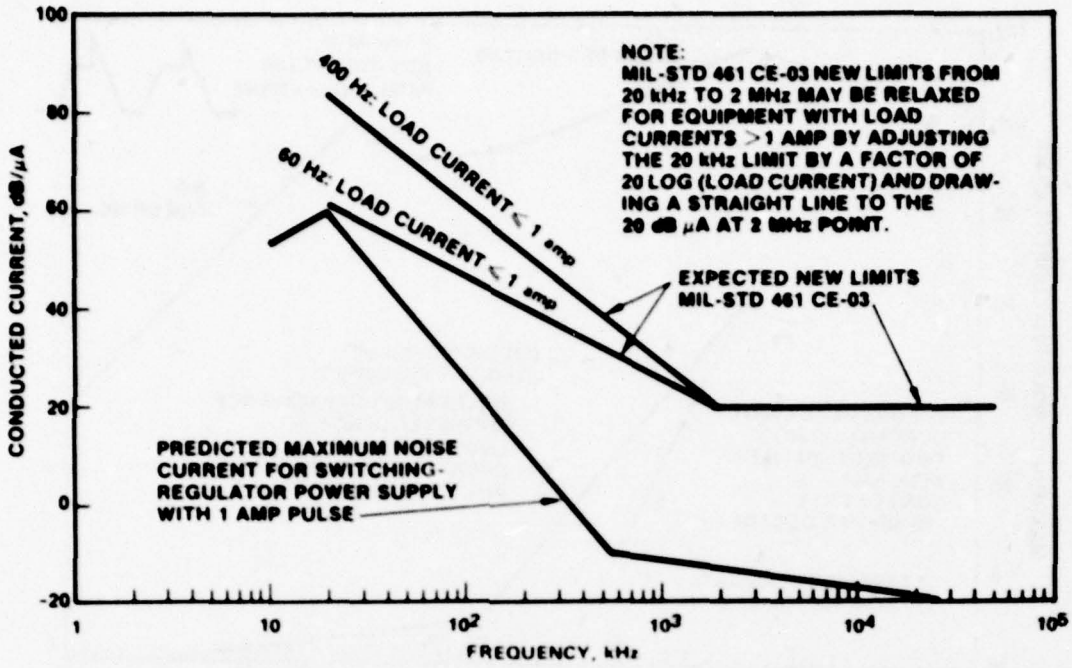

Figure 16. Predicted maximum noise current compared to expected new CE-03 Navy limits for MIL-STD 461.

Effect on Nearby Sensitive SSBN Receiving Cables

Sensitive SSBN receivers operating in the noise spectrum frequency range are potentially vulnerable to switching-regulator EMI. The EMI coupling between the receiver and the power supply can take many forms. However, of primary concern is the magnetic coupling path between the power supply input cables and the receiver input cables. Therefore, calculations were performed to determine separation distances required to prevent interference (for a range of standard Navy cables). The interference criterion included a 20-dB sensitivity safety factor in addition to the required receiver sensitivity.

Magnetic Field Emissions. In Navy electronic subsystems, the current from the power source flows through twisted-wire cables before arriving at the switching regulator power supply. This conducted input current (figure 15) sets up a magnetic field which can induce noise voltages into nearby sensitive receiver cables. To determine the magnitude of this magnetic field, models have been developed for radiation from twisted-pair lines for near and far distances.

At near distances the twisted-pair can be modeled as a parallel-wire line.

Parallel-Wire Model.[11] For parallel-wires separated at a distance d, the magnetic flux density at a distance r is:

$B \simeq \mu I/2\pi r$ for $r \ll d$,

[11] University of Pennsylvania, Moore School Report No. 74-03, "Systems Electromagnetic Compatibility Evaluation," by Showers, R. M., Dolie, K., and Conrad, T., prepared for Naval Ships Systems Command, 31 August 1973 [AD 913996], pp. 28-32.

where μ is the permeability and I is the current and

$$B \approx \mu Id/2\pi r^2 \text{ for } r \gg d.$$

Twisted-Pair Model. The maximum flux density radiated from a twisted-pair cable of pitch p and conductor separation d, a distance r away is given by Moser and Spencer.[12]

For $r \ll p/3$, use parallel wire line model

$$B = \mu_o Id/(2\pi r)(r + d)$$

and for $r \gg p/3$,

$$B = (\mu_o I/\sqrt{pr})(2\pi d/p)I_o(2\pi d/p)e^{-2\pi r/p},$$

where I is the current and $I_o(x)$ = the zeroth-order modified Bessel function of the first kind. Showers, et al. (reference 11), have provided a plot of the ratio of flux density for a twisted pair line to that of a parallel wire line as a function of r/p. This ratio may be used to estimate the maximum flux density from a twisted pair line.

Based on the preceding theoretical work (references 11 and 12), NUSC has prepared tables of flux density at various distances from standard Navy cables.[13] Data from these tables for switching-regulator-noise levels were used as one input to calculate the cable spacing requirements (receiver susceptibility data was the other input).

Representative Radiating Cable. Four different sizes of Types TSGU (three-conductor) and DSGU (two-conductor) powerline cables[14,15] were selected as representative cables radiating maximum magnetic fields encountered in the proximity of receiving cables. It was assumed either two- or three-conductor cable (maximum 1,000 volt) would be feeding typical electronic subsystems. MIL-STD-1399, Section 103,[16] specifies preferred shipboard power as ungrounded delta 440 V, three-phase, 60 Hz. (Therefore, the largest cable required is 1000-volts.)

Cable Susceptibility. The voltage induced in a cable by a magnetic field B is computed by Faraday's law:

$$V = |d\phi/dt| = 2\pi fAB,$$

where

$\phi = AB$ is the total magnetic flux linking the effective area A of the cable,

---

[12]Moser, J. R. and Spencer, R. F., "Predicting the Magnetic Fields from a Twisted-Pair Cable," IEEE Transactions on Electromagnetic Compatibility, Vol. EMC-10, No. 3, September 1968, pp. 324-329.

[13]Enclosure (1) to NUSC ltr ser 7344-38, Standard Navy Twisted Wire Cable Data, January 1977, prepared by Code 344, Naval Underwater Systems Center, New London, CT.

[14]Department of the Navy Military Specification MIL-C-915E, Cable and Cord Electrical, for Shipboard Use, General Specification for, Amendment-1, 5 April 1973.

[15]Department of the Navy, NAVSEA 0967-LP-283-5010, Handbook of Submarine Electromagnetic Shielding Practices, Section 6, Change 4, 10 November 1975.

[16]Department of the Navy Military Standard MIL-STD-1399, Section 103, Interface Standard for Shipboard Systems, Electric Power, Alternating Current, 1 December 1970.

B is the magnetic flux density assumed uniform over A,

and

f is the frequency at which V is to be calculated.

The effective area depends on the cable (reference 11, pp. 36–38). For a parallel wire line of length l and separation d,

$$A = ld.$$

For a coaxial cable of length l and eccentricity δ,

$$A = l\delta.$$

For a twisted-pair cable, a good approximation to the voltage induced is that induced in one half twist so that the effective area for a cable of pitch p and separation d would be

$$A = 2 \times 2/\pi \times d/2 \times p/2 = 0.318\ pd,$$

assuming a sinusoidal projection of the helical conductors.[17]

Two cables were chosen to represent extremes in the susceptibility range for typical Navy receiving cables. Type 2SWF typifies a less susceptible cable (twisted-wire) with an equivalent area[18] of 0.045 in^2 (0.29×10^{-4} m^2). The RG-264A/U coaxial cable was selected to represent a highly susceptible cable since it has a large effective area of 0.65 in^2 = 4.21×10^{-4} m^2 (reference 11, p. 151). Since $V = 2\pi fAB$, the sensitivity per magnetic flux density calculates to be

$V/B(dB) = 11dB\mu V/\mu T$ at 20 kHz for 2SWF cable

and

$V/B(dB) = 34dB\mu V/\mu T$ at 20 kHz for RG-264 A/U coaxial cable*

Receiver Sensitivities. Sensitivity data was obtained for receivers operating in SSBN Integrated Radio Room (IRR),[19] and sonar subsystems. (See Appendix D for some sensitivity considerations.) The data includes projected future sensitivity requirements as well as current ones.

Figure 17 shows the receiver sensitivities of those frequency ranges within the noise spectrum of the switching-regulator power supplies. The most frequently used sonar spectrum, between 3 and 10 kHz, has the same sensitivity as the frequency range shown but is below the switching-regulator noise spectrum.

---

[17] University of Pennsylvania, Moore School Report No. 71-27, Leakage and Coupling of Transmission Lines by Showers, R. M., prepared for Naval Electronic Systems Command, Technical Report No. 29, Contract N00039-71-C-0103, 15 June 1971.

[18] Nomograph for Estimating Cable Magnetic Shielding Requirements prepared by U. S. Navy Underwater Sound Laboratory (now NUSC).

[19] RCA Specification No. 8556800F Code Ident. 49671, Specification for FBM Submarine Integrated Radio Room, 1 March 1977.

*When used for VLF receivers, the RG-264A/U coaxial cable is connected internally so that it acts like a twisted pair and its sensitivity is independent of line length. This physical connection causes the large effective area.

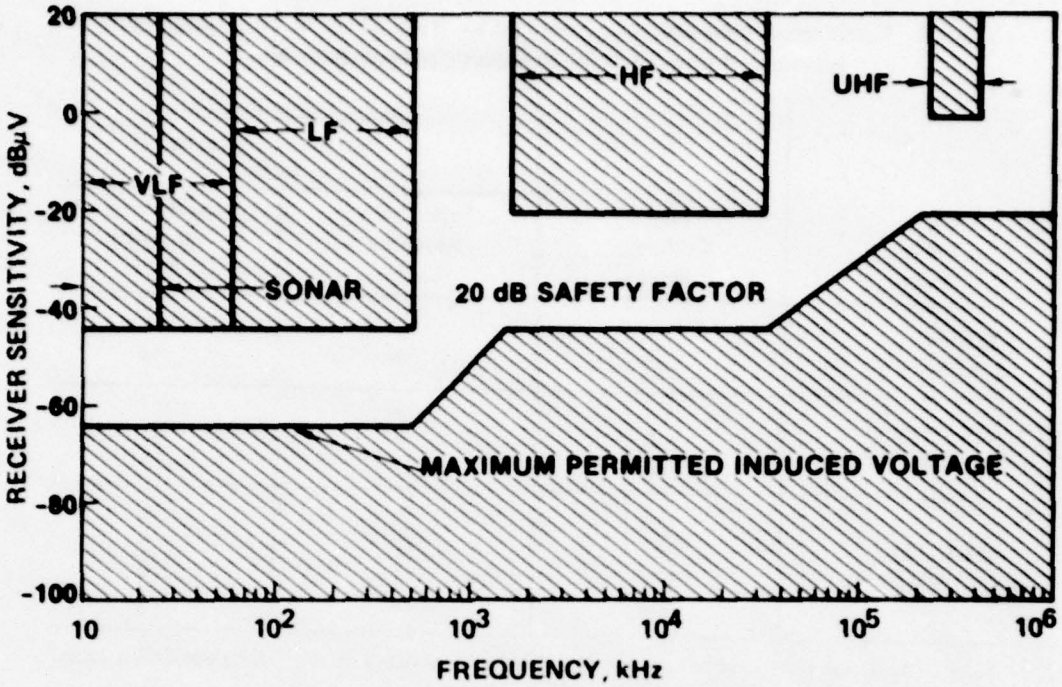

Figure 17. Receiver sensitivities.

If a 20-dB safety factor is used, then the maximum permitted induced voltage will vary from -64 dBμV at 10 kHz to -20 dBμV at 100 MHz (figure 17).

Separation Distances. Calculations* were performed to determine the interference-free separation distances required between the representative radiating power cables and the susceptible receiver cables. Details and procedures are given in Appendix E. Table 1 lists the results. For one-amp current, the less sensitive type 2SWA cable would need to be from 2 to 6 inches away from the powerline depending on the power cable size; and, for 200 amps, a 16-inch separation would be needed. For one-amp current, the more sensitive RG-264 A/U cable would need to be 3 to 10 inches away from the powerline depending on the power cable size; and for 200 amps, a 21-inch separation would be needed. No shielding was assumed for these calculations.

The IRR subsystem contains 24 racks of electronic and support equipment. Two of these racks house the VLF and LF receivers (4 in each rack) and a third rack houses the HF and VHF equipment (3 receivers). Each VLF/LF rack requires less than 9 amps of 60-Hz power and, therefore, separation distances of 3 to 15 inches may be required (table 1). However, the racks are 24 inches wide and the larger cables are unlikely to be used. Within the rack, power wiring carrying less current can be placed closer to the receiving cables. Thus the required separation distances are practical within the VLF/LF racks. A similar analysis for the HF/UHF rack indicates that required separation distances are also practical for the cables within this rack.

*Calculations were only needed at 20 kHz because the induced voltage is a maximum at that frequency. (See Appendix E for the explanation.)

Table 1. Cable spacing to preclude interference from dc-input switching-regulator unshielded power-cables to susceptible receiver cables.

Power Cable Type	Line Current, amps	Separation Between Power and Receiving Cables, inches	
		Type 2SWA Receiving Cable	Type RG-264A/U Receiving Cable
TSGU-3 (or DSGU-3)	1	2	3
	10	3	4
TSGU-100 (or DSGU-100)	1	4	7
	10	7	11
	100	11	15
TSGU-200 (or DSGU-200)	1	6	10
	10	10	15
	100	15	20
	200	16	21

Note: Distances correspond to radiated flux densities less than -75 dBμT for Type 2SWA cable and less than -98 dBμT for RG-264 A/U cable.

Outside the racks more than one power cable could be located in the vicinity of the receiving cables. Assuming all the IRR power cables were simultaneously contributing to the induction field, the resulting field would be less than a field from a cable carrying 200 amps (adding the currents statistically). As shown in table 1 for this worst condition, the separation distances required would still be reasonable, 16 to 21 inches. If the physical layout of the equipment requires closer spacing, then flexible conduct shielding can provide more than 50 dB of attenuation at 20 kHz, and higher dB values at high frequencies (reference 15).

These results show that the switching frequency and its harmonics on the input power line, if attenuated as in figure 15, are compatible with sensitive receiver circuits.

OTHER MANIFESTATIONS OF SWITCHING FREQUENCY NOISE

The discussion thus far has been limited to differential-mode powerline conducted noise which in turn causes a radiated magnetic field. Switching-frequency noise, however, can manifest itself in other ways. It is generated within wiring and non-ideal components of the power supply and can be radiated to the outside world inductively or capacitively. Also, on the output leads, a ripple voltage always exists in the form of differential-mode conducted noise.

Suppression of Internally-Radiated Noise

As indicated in several articles in recent literature, a concensus exists that EMI radiation from within the chassis is no longer a major problem. This potential noise problem has been successfully solved in recent years. In the past, switching-mode power-supply manufacturers avoided reference to EMI except for specifying output ripple. Today, however, many

low-EMI designs exist and many manufacturers* do not hesitate to refer to low EMI in their catalogs, in some cases referencing MIL-STD-461 and other governmental or industrial specifications. One manufacturer[20] states that their 27-watt power supply meets the industrial VDE** noise specification without shielding enclosures or heat sinking surfaces by providing short, low impedance return paths for noise sources and shielding the switching elements.

Several texts have recently appeared in which noise reduction techniques are discussed. Gottlieb[21] states that recent understanding of noise filtering and suppression techniques have enabled the designer to contain the spurious noise energy within the physical confines of the power supply. A book by Ott[22] is devoted exclusively to noise reduction in electronic systems and much of the detailed theoretical and practical information therein is directly applicable to switching-mode power supply noise reduction.

Some of the techniques given in these texts are discussed in Appendix F, which also discusses several recent articles concerned with EMI reduction methods for switching-mode circuits.

Ripple on Output Leads

Output ripple is an inherent characteristic of switching-mode power supplies. There is always a residual component of the switching frequency. This residual component ripple can be made arbitrarily small with filtering. Figure 2 shows a typical LC output filter. It can be designed for low output ripple and even lower ripple values are achievable with multistage filters. Very low ripple designs, however, can be expensive in component cost, and are more difficult to stabilize. Fortunately, modern day digital logic circuits have excellent noise immunity and wide switching margins. It is poor economy to over-specify power source output noise. Therefore, the maximum ripple and noise specification[23] for the recently-awarded Navy SEM power supply modules calls for ±1% of output voltages or 100 mV, whichever is greater.

A question remains: What is the most cost-effective way to deal with analog circuits that cannot tolerate such ripple? Often only one or two critical circuits require very low ripple. These sensitive circuits are best handled by adding a point-of-use series regulator. By locating the lossy regulator at the noise sensitive circuit, losses are kept at a minimum. Other circuits fed by the power supply may not need very low-ripple voltages.

---

*For example, Hewlett-Packard, Acme Electric, Gould, Conver, ACDC Electronics, Todd Products and Lambda.

**Verband Deutscher Electrotechniker (VDE) Interference Limits (West Germany) are expected to be the basis for unified limits for most European countries. The limits are given in Interference Technology Engineers Master (ITEM) 1978 published by R&B Enterprises, pp 104-105.

[20]Schimelpfenig, D. A., "The Design of the Conver 2000 Series Power Supply," paper enclosed with Conver brochure, Cupertino, CA, August 1978.

[21]Gottlieb, I., Switching Regulators and Power Supplies, Tab Books, 1976.

[22]Ott, H. W., Noise Reduction Techniques in Electronic Systems, John Wiley & Sons, 1976.

[23]Department of the Navy, Naval Ordnance System Command, NAVORD DWG Number AV21901, Power Supply Modules, Standard Electronic Module (SEM) program, General Specification for, 11 July 1977.

STRUCTURE CURRENTS

Structure currents, as discussed in a preceding report (reference 1), can create problems in sensitive VLF equipment. NUSC has conducted extensive investigations to identify,[24] to determine the causes for, and to find solutions for this problem. They found the structure currents were caused by large line-to-chassis EMI filters feeding harmonics to the structure. For example, tests on the USS GUITARRO[25] 400-Hz powerline showed that capacitive-input filter type power supplies were causing large structure currents through line-to-ground capacitors of approximately 135 μF per phase. The switching-frequency power supplies were major offenders but not primarily from their switching frequency harmonics. They were supplying excessive rectification harmonics because they used capacitive-input filters. (NOTE: In the past, it has been very common for switching-mode power supplies to be designed with capacitive-input filters. However, as discussed in the section on input filters and in Appendix C, either one or two-stage L-C filters are recommended to sufficiently attenuate the conducted switching-frequency line current.) NUSC[26] has reported that capacitive-input filters result in higher low-order rectification harmonics than inductive input filters, and recommends using inductive input filters. (Capacitive input filters also result in lower power factors requiring more system KVA than may be available.) Although rectification harmonics appear to be the major source of structure currents, switching frequency harmonics, if present, will also cause structure currents.

NUSC continues to work on this problem and some of the solutions recommended so far (reference 25) include: (a) isolation transformers, (b) line-to-line filters, (c) multi-phase transformers to reduce harmonic levels, and (d) limiting line-to-chassis capacity in EMI filters* (although where large ones already are installed it may not be advisable to change since they also reduce the rectification harmonic distortion). As discussed in the section on rectifier noise, new solutions to reduce rectification harmonics are being developed and the Delco approach appears to be particularly promising. Recently, NUSC has prepared computer programs[27] for the prediction of structure currents (caused principally by unbalanced line-to-ground impedances). Potential platforms and facilities are being investigated to validate the EMC model.

The two proposed candidate systems differ in their impact on the structure current problem and its solutions. In configuration I (figure 1), which eliminates the rectification harmonic problem, the only source of structure currents will be the switching frequency harmonics, if present, but large EMI capacitors should not be necessary if techniques discussed in Appendix F are applied. There is, however, no easy way to isolate the structure currents

---

[24] Naval Underwater Systems Center ltr 344 DSD dlm 9400 ser 7344-189 to NAVSEA and NAVSEC, subj: Common-mode and Structure Current Measurements; Definitions, Shipboard Measurement Procedure and Compendium of Shipboard Data, 20 May 1977.

[25] Naval Underwater Systems Center ltr 344 DSD dlm 9400 ser 8344-161 to NAVSEA and NAVSEC, subj: Test Results and Recommendations Resulting from Post-Overhaul EMC Measurements Conducted on the 400-Hz Powerline of USS GUITARRO (SSN 665), 5 May 1978.

[26] NUSC TM No. 771169, "Power Supply Design and Current Emissions," by G. J. Majewski, 1 August 1977.

[27] NUSC TM No. 781115, "Prediction of Ground Plane Structure Currents," by G. J. Majewski, 5 June 1978.

*Revised MIL-STD-461A specifies line-to-ground capacitance not to exceed 0.1 μF for 60-Hz equipments or 0.02 μF for 400-Hz equipments.

if they do become a problem in system integration. Configuration II (figure 1) does allow flexibility in locating isolation transformers to reduce structure currents, but at the cost of retaining the rectification harmonics and their resultant structure currents.

FUTURE LOW-NOISE DESIGNS – TWO MAJOR DEVELOPMENTS

A recently developed version of a cascaded optimum topology switching-mode power supply is a major breakthrough in reducing EMI. Also, the advent of VMOS field effect transistors (FET) has made possible duty-cycle power supplies with higher switching-frequencies easier to filter, and therefore, less EMI is easier to attain.

New Optimum Topology Configuration[28]

This novel converter (figure 18c) has the same general conversion property (increase or decrease of the input dc voltage) as does the conventional buck-boost converter (figure B-1 in Appendix B). However, its new optimum topology (maximum performance for minimum number of parts) results in reduced EMI, as well as higher efficiency, lower output voltage ripple, smaller size and weight, and excellent dynamic response. It combines the low pulsing input current of the boost converter (figure 18a) with the low pulsing output ripple of the buck converter (figure 18b). The advantages of both converters are thus combined rather than the disadvantages as in the buck-boost converter (Appendix B). Both input and

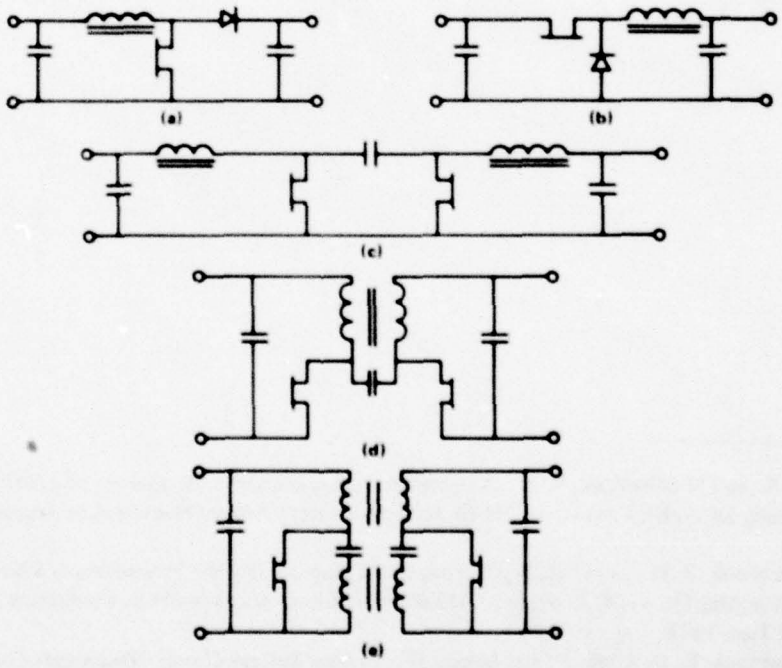

Figure 18. Optimum topology converter.

[28]Ćuk, S., and Middlebrook, R. D., "A New Optimum Topology Switching DC-to-DC Converter," paper presented at the IEEE Power Electronics Specialists Conference, Palo Alto, CA, June 1977.

output currents are not pulsating but are continuous, essentially dc with small superimposed switching current ripple.

The basic design has been extended in several aspects. In one extension,[29] the input and output inductors are combined on the same core (figure 18d) in such a way that not only are both the input and output current retained nonpulsating, but an order of magnitude or more in further reduction of either input or output current ripple may be achieved (either the input or output current ripple can be made essentially to vanish). A second extension (reference 29) uses the symmetry feature of the design to achieve both positive and negative output polarity with the same unit through true bidirectional implementation of the switch using VMOS-FET power transistors. A third extension[30] achieves dc isolation and multiple outputs (figure 18e). Another application[31] of the bidirectional characteristic (power can flow in either direction) is for battery conditioning as a charge-discharge regulator in place of conventional separate converters.

VMOS-FET Higher-Frequency Power Supplies

As was discussed previously, increasing the switching-frequency can result in more attenuation for given size filter components (or smaller components for the same attenuation). The primary drawback — degradation of efficiency due to increased switching losses — has been largely overcome by the application of VMOS switching devices.[32] It is anticipated that as VMOS technology matures, operation at 100 kHz and beyond will become more commonplace.

---

[29] Ćuk, S., and Middlebrook, R. D., "Coupled-Inductor and Other Extensions of a New Optimum Topology Switching DC-to-DC Converters," IEEE Industry Society Annual Meeting, Los Angeles, CA, 2-6 October 1977.

[30] Middlebrook, R. D., and Ćuk, S., "Isolation and Multiple Output Extensions of a New Optimum Topology Switching DC-to-DC Converter," IEEE Power Electronics Specialists Conference, Syracuse, NY, 13-15 June 1978.

[31] Middlebrook, R. D., Ćuk, S., and Behan, W., "A New Battery Charger/Discharger Converter," IEEE Power Electronics Specialists Conference, Syracuse, NY, 13–15 June 1978.

[32] Shaeffer, L. (Siliconix, Inc.), "Improving Converter Performance and Operating Frequency with a New Power FET," paper presented at POWERCON-4, Boston, Mass., May 1977.

PRELIMINARY COST-BENEFIT STUDIES

A Business Week article[33] states that "switching technology is edging linear products out of the $2 billion market" in power supplies. "Switching components are dropping in price, and new integrated circuits (ICs) are consolidating many control functions into one device." As a result, "switching supplies have been growing 30 to 35 percent annually for the last four years. By 1980, sales of switchers are expected to reach $553 million, which would double their current market share."

A new power supply company was started recently because two years of market research[34] showed an "enormous potential market for switching-regulator power supplies," and that "within the last two years, switcher manufacturers have solved the reliability, cost and RFI problems that plagued early designs."

As these quotations from recent literature indicate, the advantages are considerable. These advantages will benefit electronics systems of existing and future SSBN submarines if one of the proposed candidate approaches (figure 1) are implemented. Configuration I, however, will reap an additional benefit by eliminating the ac-to-dc converter(s).

To determine the magnitude of these benefits for SSBN submarines, work was initiated to assess the costs and benefits of using dc-input switching-mode power supplies in a typical electronic subsystem. The Integrated Radio Room (IRR) subsystem was selected.

To date, initial studies have compared dissipative and switching-mode power supplies in acquisition costs, operating energy requirements, weight, and volume. These study results will be one of the inputs to the cost-benefit study for the IRR subsystem. Also other costs and benefits will be assessed if applicable.

Although considerable information was obtained about the IRR electronic equipment, FY 79 plans are to seek additional parametric data.

ACQUISITION COSTS, OPERATING ENERGY COSTS, AND WEIGHT

Table 2 compares the cost of switching-mode power supplies to 60 and 400 Hz dissipative power supplies from the same manufacturer's catalog. The switching-mode power supplies weigh the least, cost the least, and use almost 50 percent less energy.

VOLUME

The impact of power conversion efficiency can be illustrated by comparing the relative volume occupied by the load and the power conversion subsystem under equal thermal density conditions, i.e., identical cooling and component temperatures. The relative volumes for different efficiencies are shown in table 3. The volumes are proportional to relative power consumption, cooling requirements, volume and weight. They are also sometimes proportional to cost and failure rate. The efficiency is not arbitrary but reflects the typical efficiencies to convert shipboard electrical power to 5-V dc. The first three efficiencies represent

---

[33] An Electrifying New Market in Power Supplies, an article in Business Week, October 31, 1977.
[34] Small, C., Former AMS Head Starts Power Supply Firm, Electronic Engineering Times, July 10, 1978.

Table 2. Power supply comparisons.[a]

Type	Cost, $	Weight, lb	η, %	Pout, W	Pin, W	Energy/Year[c] kWh
60 Hz Dissipative[b]	1,450	80.5	35	300	857	7,507
400 Hz Dissipative[c]	1,644	26.7	35	300	857	7,507
Switching-Mode[d]	1,239	16.2	65	300	462	4,043

Switching Mode Power Supplies Savings

Acquisition Cost Savings	$211 to $405
Energy Savings Per Year	3,464 kWh
Weight Saving	10.5 to 64.3 lbs

Notes:

[a]Sealed power supplies from Abbott Transistor Laboratories Power Supply Catalog 1977-78.
[b]Model V6DS-5A (5V-12A) 5 units @ $290 each.
[c]Model W5D20 (5V-20A) 3 units @ $548 each.
[d]Model VN100D-5A (5V-20A) 3 units @ $413 each.
[e]8,760 h/year.

Table 3. Power supply volume versus efficiency.

Efficiency, %	Load Volume, units	Power Supply Volume, units	System Volume Occupied by Power Supply, %
22	1	3.55	78
27	1	2.70	73
35	1	1.86	65
65	1	0.54	35
80	1	0.25	20

dissipative regulators. Twenty-two percent efficiency is typical of submarines for electronics using 400-Hz power, 27 percent efficiency is typical of surface ships for electronics using 400-Hz power, 35 percent efficiency is typical of submarines and surface ships for electronics using 60-Hz power and for aircraft. An efficiency of 65 percent is typical of present day switching-mode power supplies operating from the platform primary power source. Eighty percent efficiency is within present technological limits. The advantage of using highly efficient power conversion in reducing size and weight of electronic systems is illustrated by table 3 and by previous studies where the issue is discussed (reference 2).

SSBN INTEGRATED RADIO ROOM

Data were obtained on the physical characteristics of the 24 IRR subsystems (including estimates for growth equipment). The data included the following parameters:

- weight,
- width, depth and height,
- deck load (lbs/ft^2),
- connected load (watts at the various line voltages), and
- cooling load (both water and air watts).

An inventory and description of the equipment in each subsystem, and for some equipment, specific power supply data were also obtained. Additional information will be sought in FY 79.

FY 78 RESULTS AND CONCLUSIONS

The study of electrical noise in switching-mode power supplies yielded designs compatible with sensitive circuits. Specific results and conclusions are as follows:

a. Switching-frequency fundamental and harmonics on the input power line can be sufficiently attenuated to be compatible with sensitive receiver circuits, even those operating in the same frequency range.

b. State-of-the-art switching-mode power supplies can be designed to meet the expected new Navy CE-03 limits for MIL-STD-461A.

c. Internally-radiated noise is no longer a major problem. Noise reduction techniques must be used; and as they are being used successfully, information about them is available.

d. Ac-powered switching-mode power supplies decrease line rectification harmonics to the extent that they conserve power, which for 5-V supplies is about one-half the amplitudes obtained with dissipative power supplies. To achieve further attenuation, several methods exist and new, better approaches look promising. Dc-powered switching-mode power supplies eliminate rectification harmonics.

e. Output ripple is an inherent characteristic of switching-mode power supplies. The most cost effective way to deal with intolerant sensitive analog circuits (usually only a few require very low ripple) is by adding a point-of-use regulator.

f. A major breakthrough in reducing EMI is a recently developed optimum topology switching-mode power supply. Both the input or output current ripple at the switching frequency can be made essentially to vanish. Further development of resonant converters and VMOS will also result in reduced EMI converters.

Initial cost-benefit studies show that, compared to dissipative power supplies in submarines, low-voltage switching-mode power supplies occupy 1/7 to 1/3 the volume, weigh 1/5 to 1/2 as much, use half the energy – and are 15 to 25 percent less expensive.

RECOMMENDATIONS

The conclusion that switching-mode power supplies are compatible with sensitive communication circuits answers a key question raised in the FY 77 study. A roadblock to the proposed candidate system is eliminated. Therefore, continuation of this study is recommended to the point where sufficient information for a decision is available. As a follow-on effort, the following activities should be performed:

1. Complete the assessment of costs and benefits of using dc-input switching-mode power supplies in the IRR subsystem.

2. Conceive a system design based on the proposed configuration, identifying components and subsystems that need major development.

3. Obtain additional data on measured EMI from switching regulators.

APPENDIX A. FOURIER TRANSFORMS

FOURIER TRANSFORM FOR TRAPEZOIDAL WAVEFORMS

Periodic Waveform

By Fourier analysis the amplitude at the frequency of the n^{th} harmonic, C_N, of the symmetrical trapezoidal periodic pulse (figure A-1) is

$$C_N = 2A \frac{(t_O + t_r)}{T} \cdot \frac{\sin[\pi n(t_O + t_r)/T]}{\pi n(t_O + t_r)/T} \cdot \frac{\sin(\pi n t_r/T)}{\pi n t_r/T} \qquad (1)$$

For $t_O + t_r = T/2$, C_N is plotted in figure A-2 for lower order harmonics (assuming $[\sin(nt_r/T)]/(nt_r/T) = 1$ which is true for small values of nt_r/T). This is the same result that would be obtained for a square wave where only odd harmonics are obtained.

Modified Three-Phase Waveform

For three-phase rectification with no transformer or with a delta-delta transformer, the line current waveform can be represented by figure A-3.

A Fourier analysis of a similar waveform (assuming $t_r = 0$) is shown by Schaefer[A1] to result in all odd harmonics except for n = 3, 6, 9, etc., with the same amplitudes as for the square wave (figures A-4(a) and (b)). Since the low frequency harmonic spectrum is the same for both the rectangular and trapezoidal pulses the harmonics relationships shown in figure A-4(a) and (b) also apply to (c) and (d).

For $t_O + t_r < T/2$, C_N is plotted in figure A-5 for lower-order harmonics. This is the same result that would be obtained for a rectangular pulse.

Envelope Approximation of Harmonics

The envelope of the low-ordered harmonics is actually a sin x/x function (see figure A-5). A linear envelope, however, can be obtained by using a logarithmic frequency scale as shown in figure A-6.[A2] The negative amplitudes of the sine function are inverted since only magnitudes are considered. Figure A-6 depicts the spectrum obtained for a single pulse ($T \to \infty$) and, therefore, amplitudes are per megahertz bandwidth (broadband classification). If coherent[A3] broadband amplitudes exist, then a definite relationship exists between

---

[A1] Schaefer, J., Rectifier Circuits, pg. 294-302, John Wiley, 1965.

[A2] Figures A-6 through A-10 are from U. S. Army Electronics Laboratories, Interference Reduction Guide for Design Engineers, Vol 1 prepared by Filtron Co. under Contract DA-36-039SC-90707, 1 Aug 1964 with permission of Filtron Co.

[A3] "A signal or emission is said to be coherent when neighboring frequency increments are related or well defined in both amplitude and phase" from White, D., Electromagnetic Interference and Compatibility, Vol 2, pg. 235, Don White Consultants, 1976.

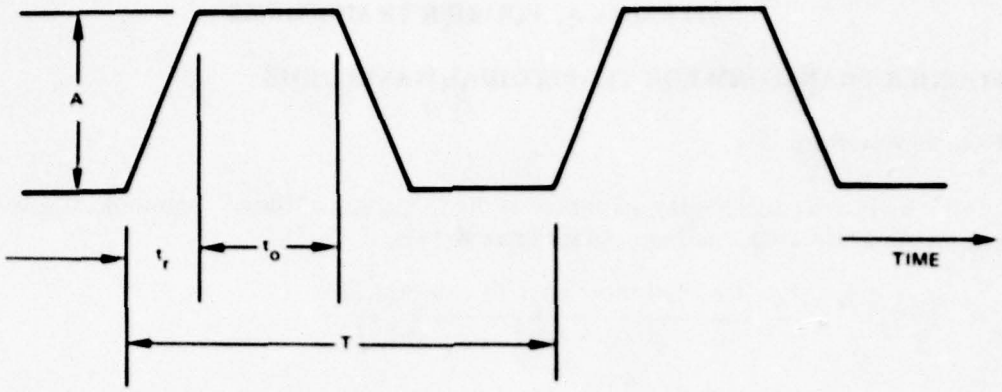

Figure A-1. Symmetrical trapezoidal periodic waveform.

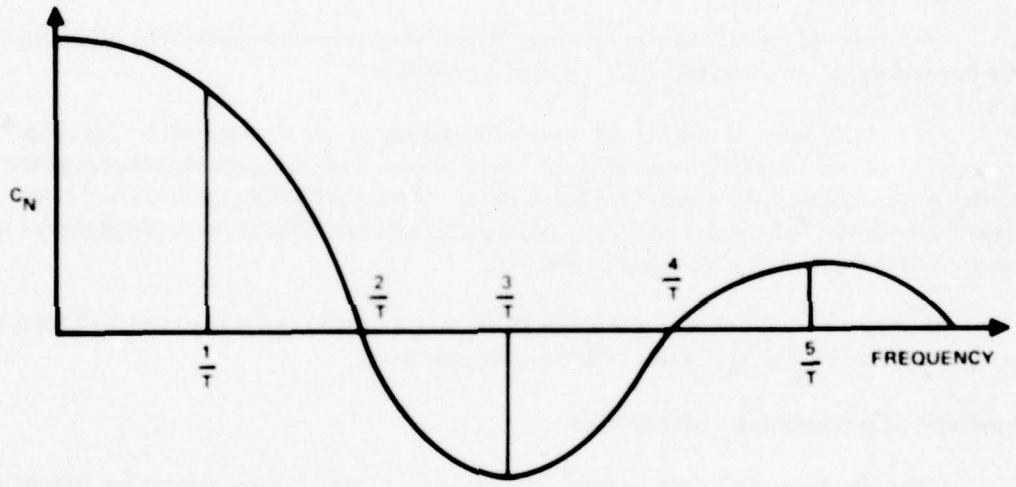

Figure A-2. Low frequency harmonic spectrum for $t_r + t_o = T/2$ trapezoidal pulse.

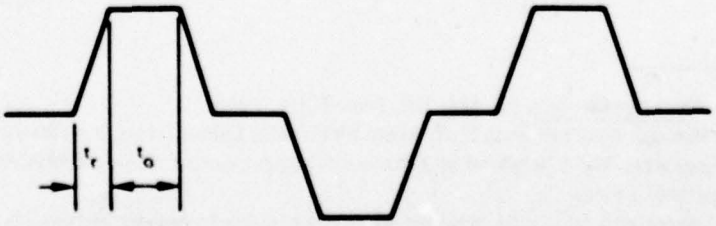

Figure A-3. Three phase rectification waveform.

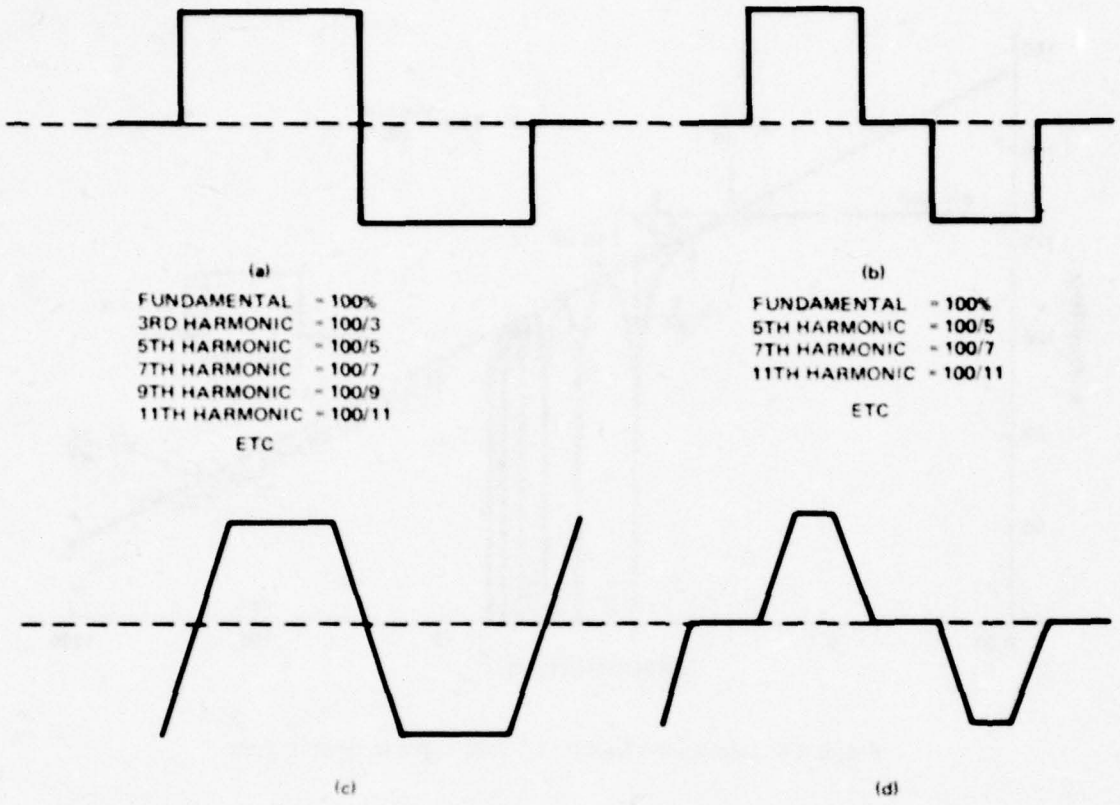

Figure A-4. Low frequency harmonic comparison for rectangular and trapezoidal waveshapes.

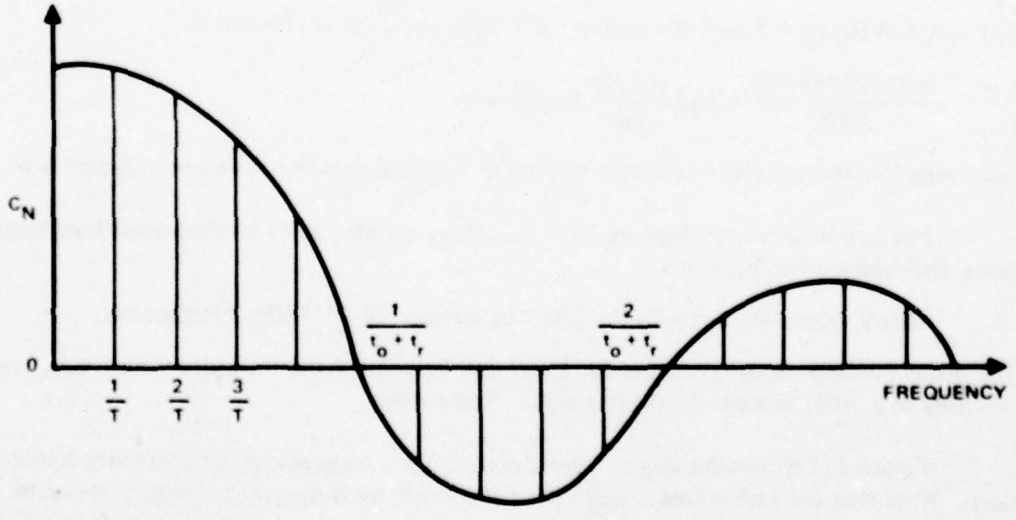

Figure A-5. Low frequency harmonic spectrum for trapezoidal pulse.

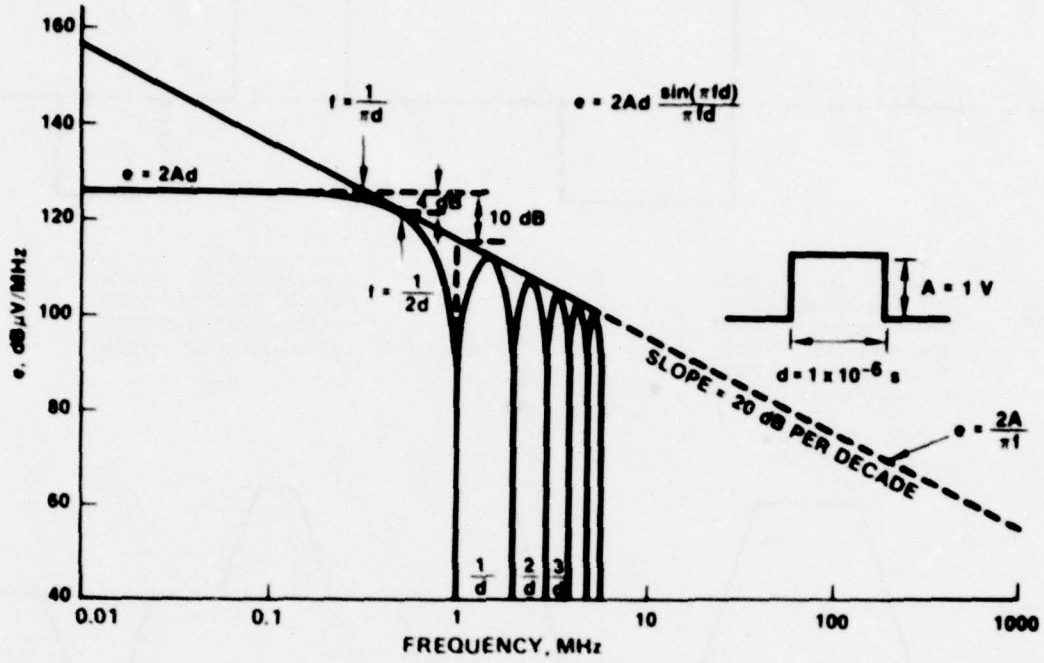

Figure A-6. Interference level for a 1-volt, 1-μsec rectangular pulse.

narrowband and coherent broadband amplitudes. By dividing equation (1) by the pulse repetition rate (PRR), an amplitude per PRR is obtained. But

$$PRR = \frac{1}{T},$$

$t_o + t_r = d$ in figure A-5, and if f replaces n/T then equation (1) becomes:

$$\frac{\text{narrowband } C_N}{PRR} = 2Ad\,\frac{\sin \pi fd}{\pi fd} \text{ broadband},$$

(assuming low frequencies where $(\sin \pi ft_r)/\pi ft_r \approx 1$) which is the equation in figure A-6.

For amplitudes expressed in dB (e.g., μV, as in figure A-6) and bandwidth in megahertz, the relationship becomes

dB/μV (narrowband) – 20 log (PRR in MHz) = dB/μV/MHz (broadband).

The linear envelope approximation for a rectangular pulse varies inversely with frequency resulting in a 20-dB decade-decreasing slope (figure A-6).

Figure A-7 shows the linear approximation for a trapezoidal pulse in three linear sections. Note that for higher frequencies the pulse rise time is more significant and results in a 40-dB per decade decreasing slope. Slower risetimes produce less high frequency interference. For periodic pulses, the lowest frequency that would appear would be 1/T or the pulse repetition rate.

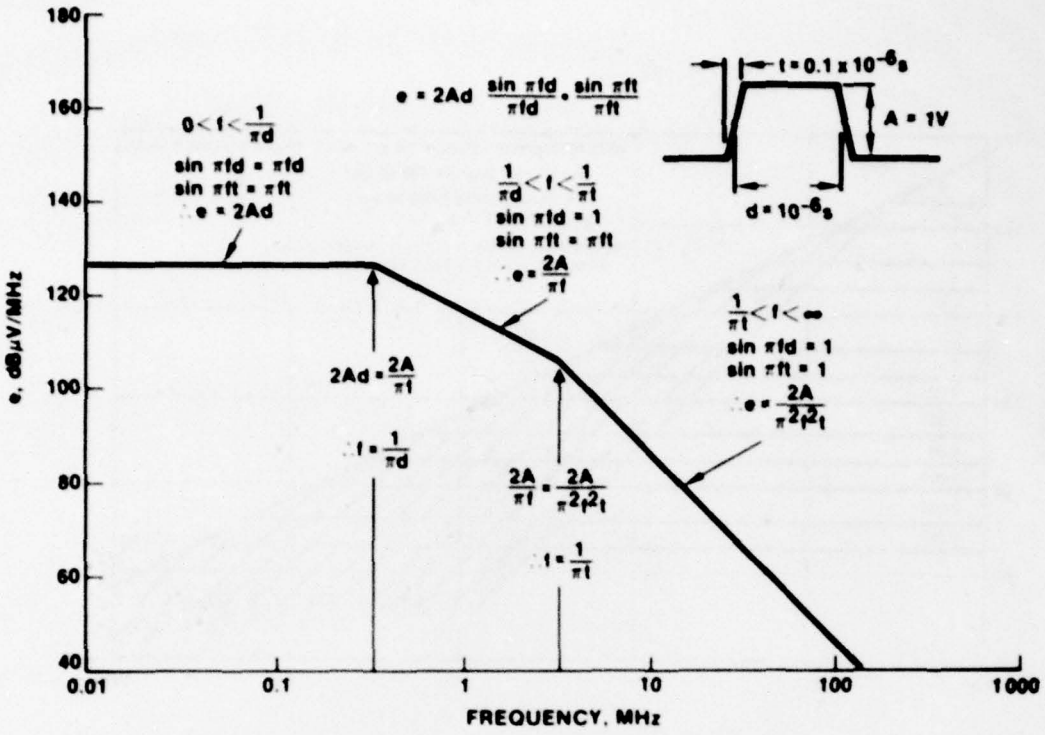

Figure A-7. Interference level for a 1-volt, 1-μsec trapezoidal pulse.

The interface levels for any trapezoidal pulse are given on figure A-8. The area under the pulse, maximum amplitude of the pulse, and rate of rise of the pulse define the envelopes of interference in the three frequency regions. The average pulse duration and the pulse rise time determine the corner frequencies.

ENVELOPE APPROXIMATIONS FOR COMMON PULSE SHAPES

The loci of maximum amplitudes for eight common pulse shapes are shown on figure A-9. All have a one-volt peak amplitude and an average pulse duration of 1 μsec. Because all of the pulses have the same area, the interference levels at low frequencies are identical. At frequencies less than 1/d, the interference level equals 2Ad or 126 dB above a μV per MHz. Above a frequency of approximately 1/d, the interference level drops at a rate determined by the shape of the rise and fall time of the pulse. For a rectangular pulse or a clipped sawtooth pulse (both of which have step functions), the spectrum extends to higher frequencies; it decreases as the first power of frequency, or at a 20-dB-per-decade rate. For a trapezoidal pulse, a critically damped exponential pulse, a triangular pulse, and a cosine pulse (all of which have sharp corners), interference decreases as the second power of frequency or at a 40-dB-per-decade rate. For a cosine-squared pulse, which has small corners, the interference decreases as the third power of frequency or at a 60-dB-per-decade rate. For a Gaussian pulse, the smoothest pulse considered, the interference drops at a rate that increases with frequency.

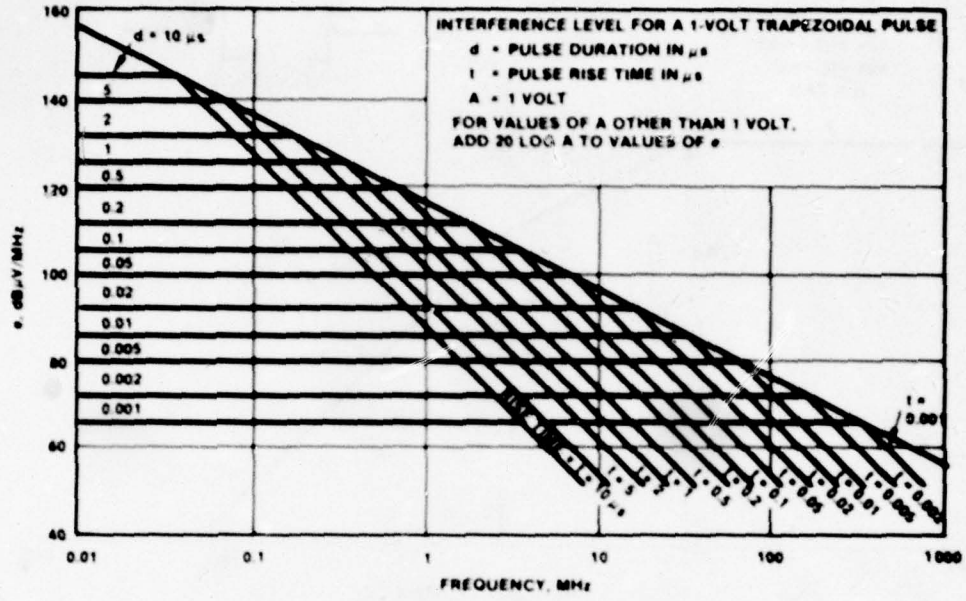

Figure A-8. Trapezoidal pulse interference.

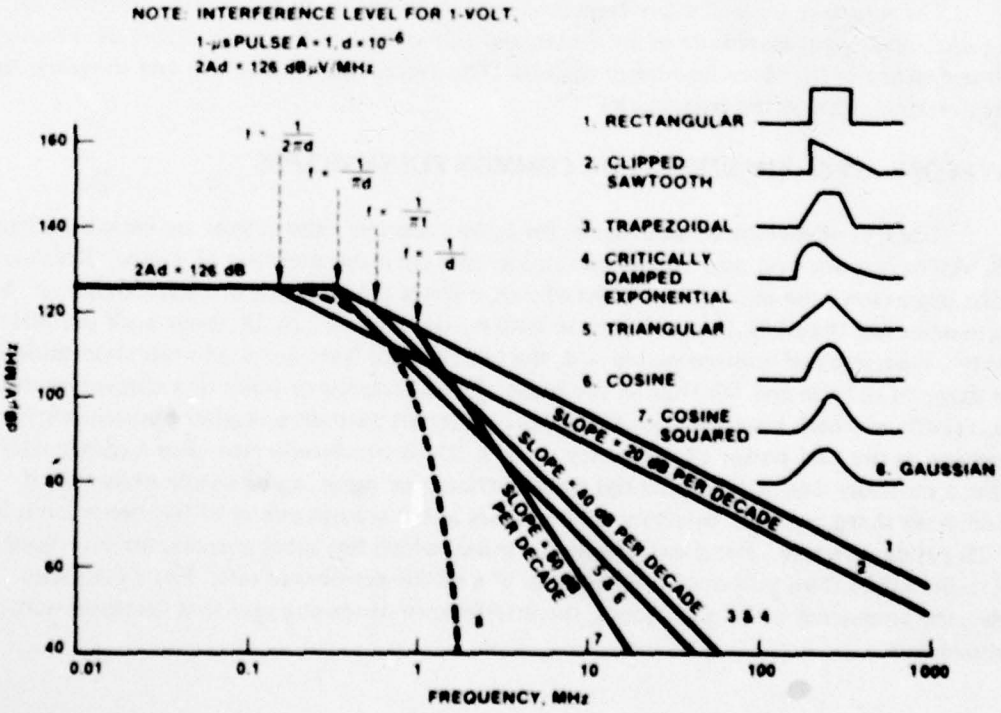

Figure A-9. Interference levels for eight common pulses.

The curves on figure A-10 are identical to those on figure A-9, but the ordinate and abscissa scales have been changed so that the curves can be applied to a pulse of any voltage amplitude and any pulse duration. The ordinate gives the number of decibels below 2Ad, and the abscissa is plotted in frequency in terms of 1/d. To find the interference level of any pulse, calculate 2Ad from the peak pulse amplitude and the average pulse duration and select the curve which most nearly resembles the given pulse shape. This curve will give the number of decibels below 2Ad for any frequency.

Although the pulse shapes analyzed here are ideal, the same methods may be used for other waveshapes by considering the waveshape to be made up of a number of rectangular and triangular pulses. For any pulse shape, the interference level at low frequencies depends only on the area under the pulse; at high frequencies, the level depends on the number and steepness of the slopes. The curves on figure A-10 are the envelopes of the frequency lobes, each lobe being an envelope of the harmonic lines that make up the frequency spectrum. Although the true curves have numerous sharp nulls, the envelope is less than 3 dB from the average interference level and represents the worst case of maximum interference level.

FOURIER TRANSFORM OF "RINGING"

A damped sinusoid "ringing" waveform is described by:

$$f(t) = ae^{-\alpha t} \sin \beta t,$$

then the frequency domain is given by

$$C_N = -\frac{1}{\frac{2\alpha}{a} + j\frac{(\alpha^2 + \beta^2 - \omega^2)}{a\omega}},$$

where $\omega = 2\pi f$ and a, α and β are coefficients necessary to satisfy f(t) functions.

Figure A-11 is an example of the loci of maximum frequency amplitudes for a damped sinusoid. Note that it peaks at a slightly higher frequency than the ringing frequency and then drops off at 40 dB per decade. Here again, if this waveform were periodic, the lowest frequency that would appear would be 1/T or the PRR.

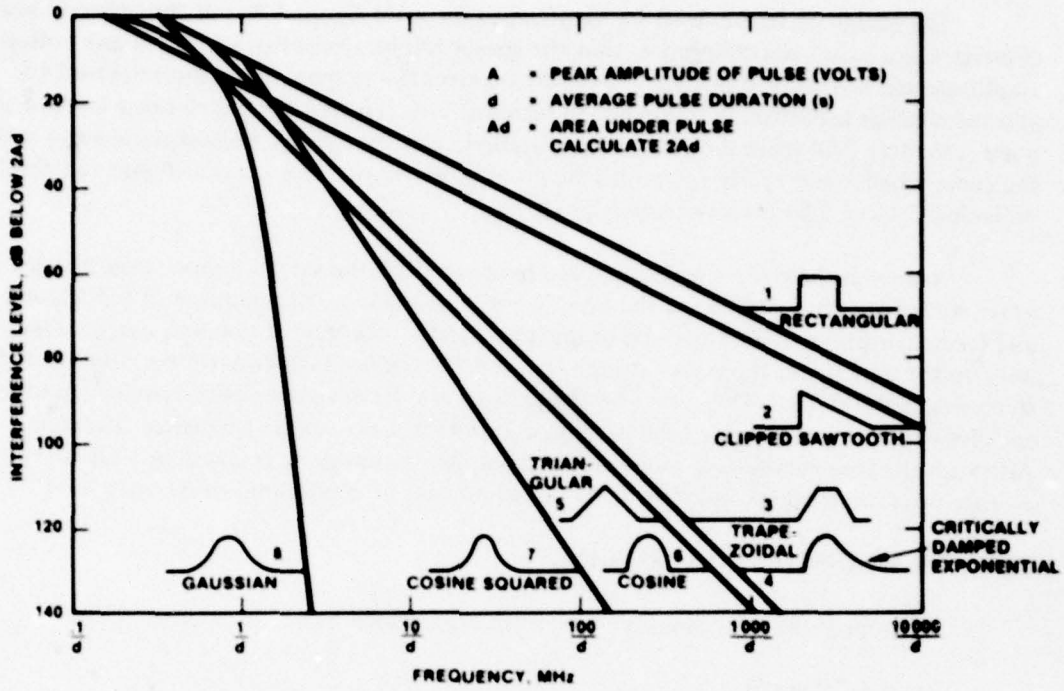

Figure A-10. Interference levels for various pulse shapes.

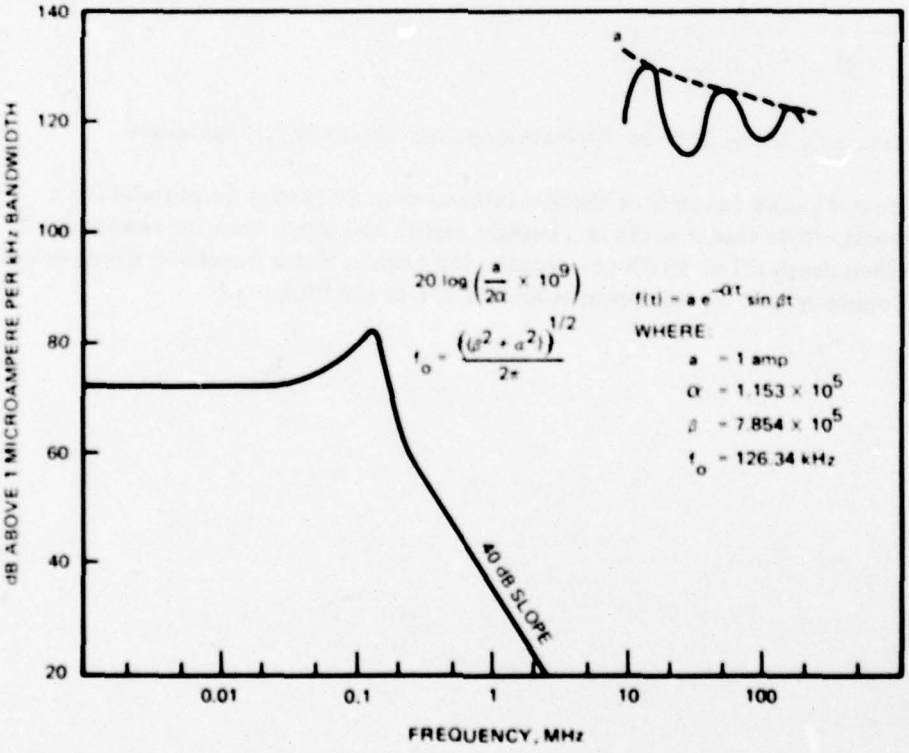

Figure A-11. Normalized frequency spectrum of damped sinewave pulse.

APPENDIX B. INPUT AND OUTPUT WAVEFORMS FOR THREE TYPES OF SWITCHING-MODE POWER SUPPLIES

Figure B-1* depicts input and output waveforms for three types of switching-mode power supplies. Waveforms are shown for both continuous and discontinuous modes of operation (discontinuous inductor current occurs at light load conditions). Figure B-2 shows waveforms for the transition point between continuous and discontinuous modes. The same output voltage (V) is assumed for all three models and, therefore, the input voltages are different (2V for the buck, V/2 for the boost and V for the buck-boost).

Under these conditions it appears that the buck-boost results in more input-conducted EMI than the buck. A more realistic comparison is to assume intervening transformers and the same input voltages (figure B-3). The input currents then have identical waveforms.

To summarize the results for the three models given the same input voltages (and intervening transformers) the following generalities hold true:

a. A buck switching-mode power supply distorts the input current more severely than the boost type.

b. A boost switching-mode power supply results in higher output ripple voltage than the buck type.

c. A buck-boost switching-mode power supply produces the buck's distorted input current and the boost's output ripple — combining the disadvantage of each.

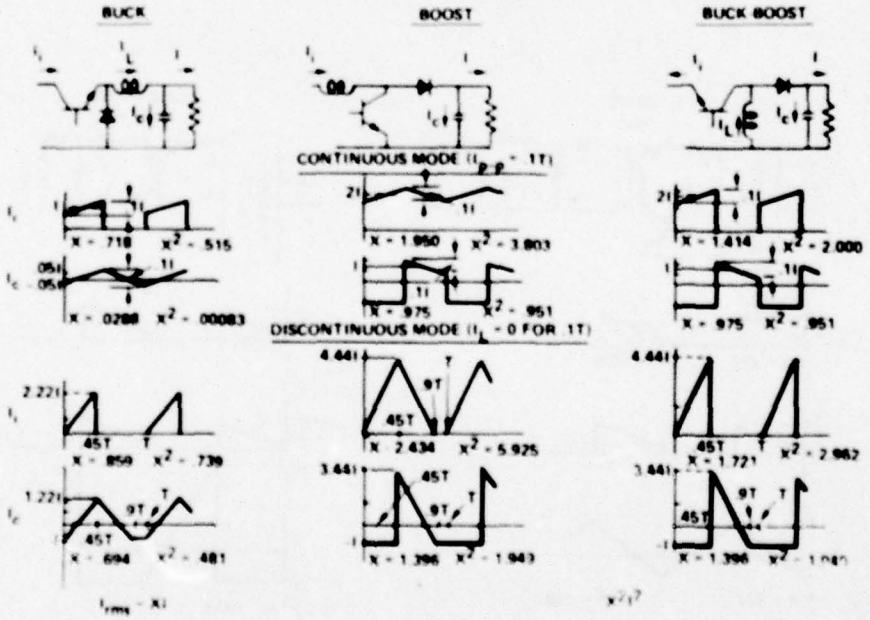

Figure B-1. Switching-mode power supply current waveforms for continuous and discontinuous modes.

*Figures B-1, B-2, and B-3 were generated by Mr. Carl W. Rosengrant, NOSC Code 9234.

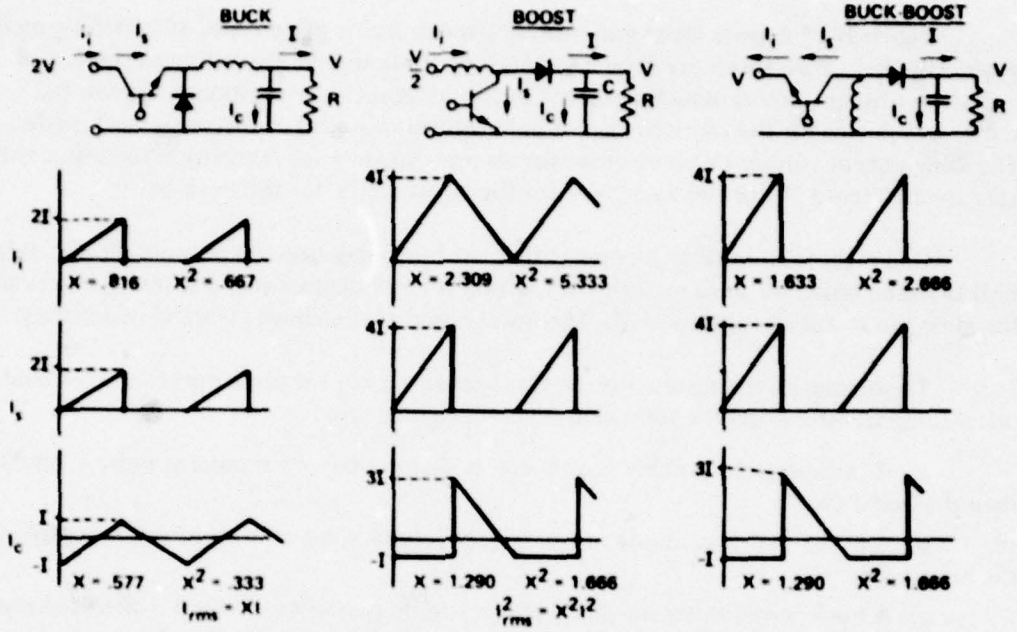

Figure B-2. Switching-mode power supply current waveforms.

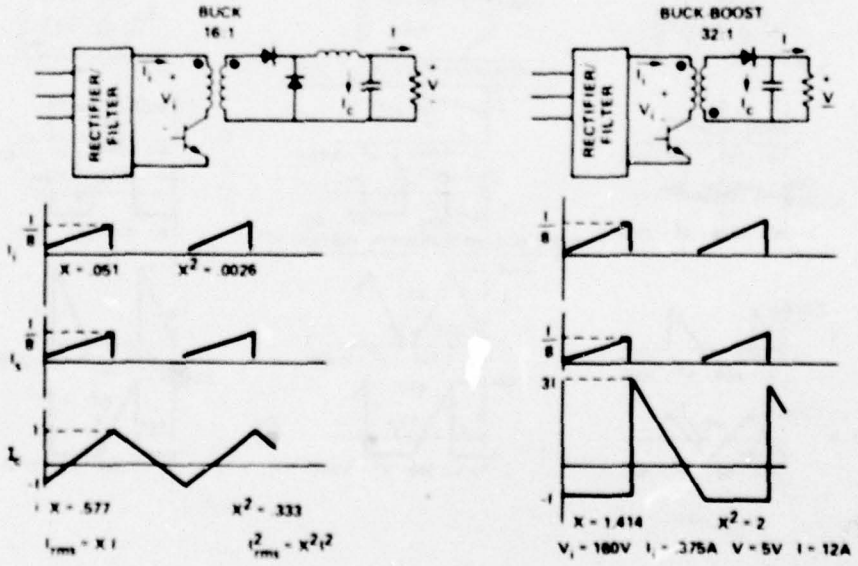

Figure B-3. Transformer coupled buck and buck-boost switching-mode power supplies.

APPENDIX C. INPUT (EMI) FILTER IN DC-TO-DC SWITCHING-MODE POWER SUPPLIES

INTRODUCTION

Switching-mode regulators require an input filter to smooth the current drawn from the unregulated line supply. The input filter, however, can cause instability because switching-regulators have a negative input resistance at low frequencies. Middlebrook[C1] treats the problem in a general manner for all forms of switching-converters, and develops criteria for input resonant frequency and Q that ensure system stability. In his paper he analyzes and gives criteria for several types of single-section input filters and also one possible two-section filter. Higher attenuation is more readily achievable with this two-section filter. A two-section filter is also more cost effective. This is demonstrated by Yu, et al.,[C2] who have formulated a design optimization methodology for switching-regulator components and circuits. In the following paragraphs, two of these optimum designs are analyzed graphically to demonstrate their attenuation characteristics. Two other related topics are discussed. One is the effect of non-ideal capacitors and the second is a method of lossless resonant damping.

MIDDLEBROOK'S ANALYSIS AND CRITERIA

The switching-mode converter acts as a dc transformer having some voltage conversion ratio $\mu = V_s/V$ (figure C-1). Assuming 100-percent efficiency (switching regulators are highly efficient), the current conversion ratio is $I_i/I = 1/\mu$ and the converter input power $P = V_s I_i$ equals the output power VI. The regulator adjusts μ to maintain constant output voltage and hence constant output power, even if V_s varies. Thus if V_s increases, I_i must decrease since input power also remains constant resulting in a negative incremental input resistance R_i given by

$$R_i = dV_s/dI_i = dP/dI_i = -\mu^2 R.$$

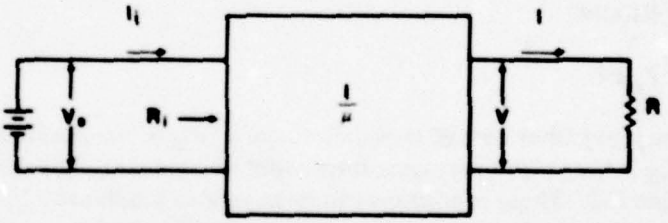

$$V = \frac{1}{\mu} V_o$$

$$I = \mu I_i$$

$$R_i = -\mu^2 R$$

Figure C-1. Switching mode power supply as a dc transformer.

[C1] Middlebrook, R. D., "Input Filter Considerations in Design and Applications of Switching Regulators," paper presented at the IEEE Industry Applications Society Annual Meeting, Chicago, October 1976.

[C2] Yu, Y., Backmann, M., Lee, F. C. Y., (TRW Defense and Space Systems) and Triner, J. E., (NASA Lewis Research Center), "Formulation of a Methodology for Power Circuit Design Optimization," paper presented at IEEE Power Electronics Specialists Conference, Cleveland, OH, June 1976.

This regulator negative input resistance R_i in combination with the input filter can, under certain conditions, cause system instability. Stability, however, can be assured by adhering to two design inequalities as explained in the following paragraphs.

Equivalent Circuit of the Switching Regulator

A generalized small-signal linear model is developed and is represented by the bottom configuration in figure C-2. The generalized model represents either the buck, boost, or buck-boost configuration by inserting the expressions indicated in the table for the parameters in the general converter model. In each case, V_S and D represent the steady state (or dc) input voltage and duty ratio, and V, the dc-output voltage. The lower case letters, v_S, d and v are their small signal ac counterparts. The model is based on averaging techniques whereby the model for the transistor-on diode-off time period is averaged with the model for the transistor-off-diode-on time period. The figures directly beneath the three basic converter stages represent the two different time periods – the left one in all cases being the transistor-on diode-off period. The generalized model represents, with appropriate expressions for the parameters, any dc-to-dc converter including not only the three basic configurations; it is subject only to the constraint that the converter operates in the "continuous" (or "heavy") mode in which the inductor current does not fall to zero at any time. The resistance R_e is an "effective" resistance of various component resistances and also of the duty ratio whose principal effect is on the Q-factor of the averaging L_eC filter.

The addition of an input filter (figure C-3) degrades the performance of a switching regulator by lowering the loop gain (T), raising the line transmission factor (F) and raising the output impedance (Z_O). These performance factors will be minimally affected if certain criteria are adhered to.

Stability is ensured (keeping T and F essentially unaffected) if

$$|Z_s/\mu^2 Rf(s)| \ll |1| \tag{1}$$

$$|Z_s/\mu^2 Z_{ei}| \ll |1| \tag{2}$$

where Z_S is the input filter output impedance, and $\mu^2 Z_{ei}$ is the regulator open-loop input impedance (Z_{ei} is the output averaging filter input impedance). The other parameters are defined in figure C-2. These conditions can be examined graphically by looking at figure C-4. First, the expression for closed loop input impedance (Z_i) can be expressed as

$$\frac{1}{Z_i} = -\frac{T}{1+T} \cdot \frac{1}{\mu^2 Rf(s)} + \frac{1}{1+T} \cdot \frac{1}{\mu^2 Z_{ei}}.$$

At dc and low frequencies where the loop gain T is large, the first term dominates and

$$Z_i \simeq -\mu^2 Rf(s).$$

However, above loop-gain crossover where T falls below unity, the second term dominates and

$$Z_i \simeq \mu^2 Z_{ei}.$$

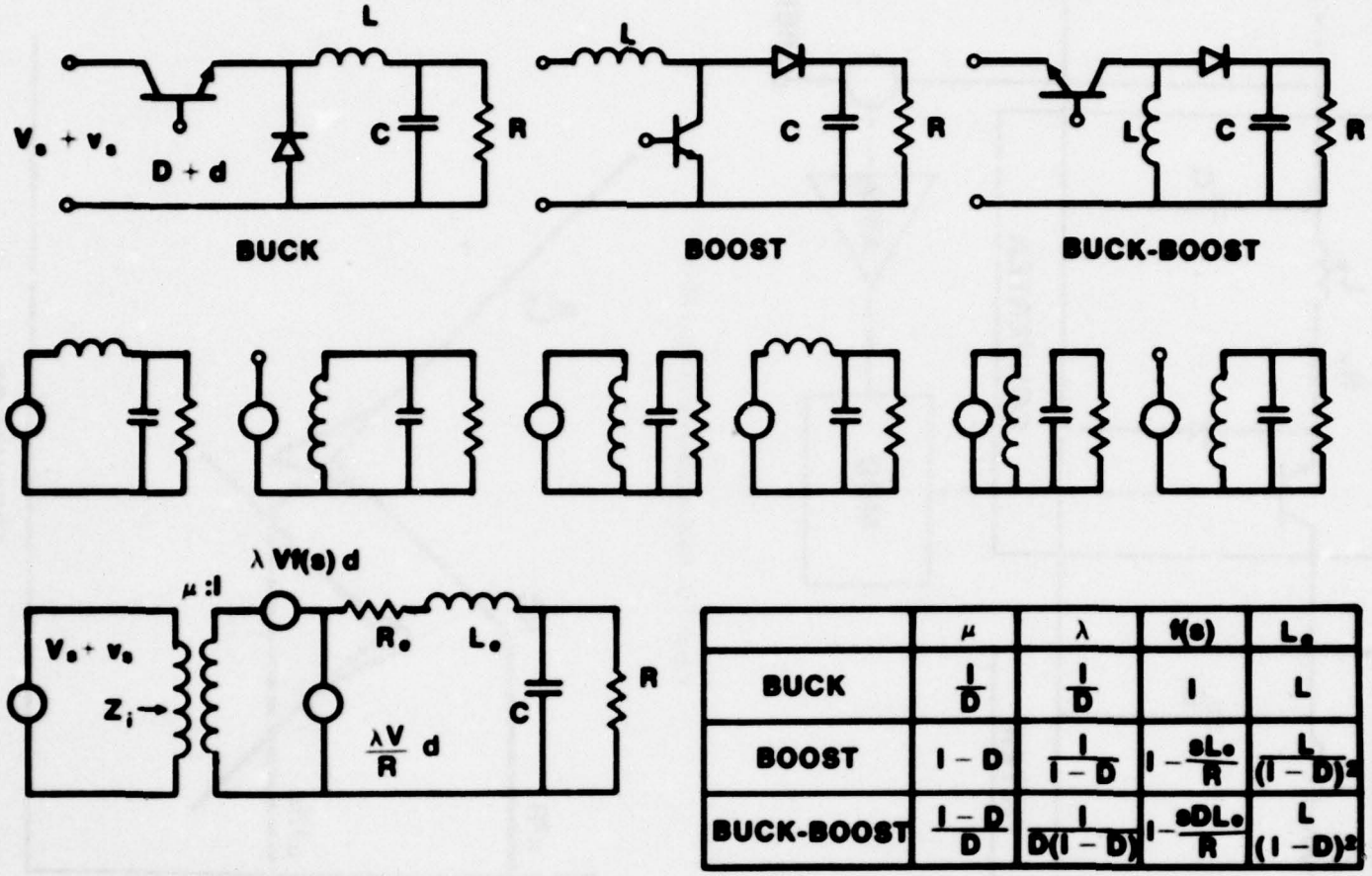

	μ	λ	$Y(s)$	L_o
BUCK	$\frac{1}{D}$	$\frac{1}{D}$	1	L
BOOST	$1 - D$	$\frac{1}{1 - D}$	$1 - \frac{sL_o}{R}$	$\frac{L}{(1 - D)^2}$
BUCK-BOOST	$\frac{1 - D}{D}$	$\frac{1}{D(1 - D)}$	$1 - \frac{sDL_o}{R}$	$\frac{L}{(1 - D)^2}$

Figure C-2. Basic switching mode power supply configurations.

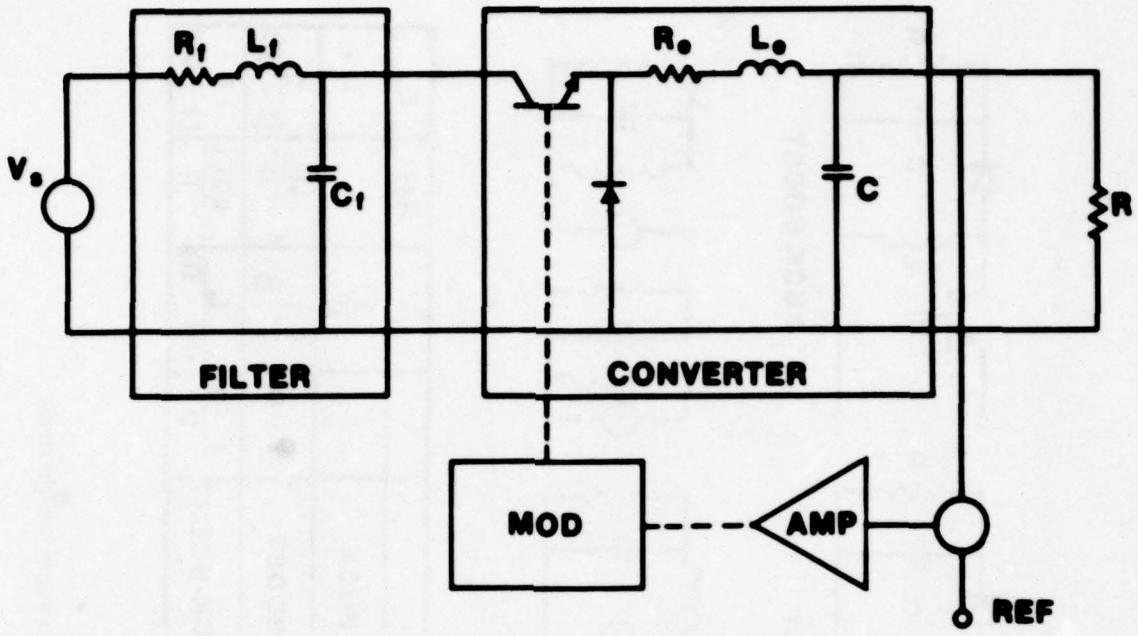

Figure C-3. Buck regulator with input filter.

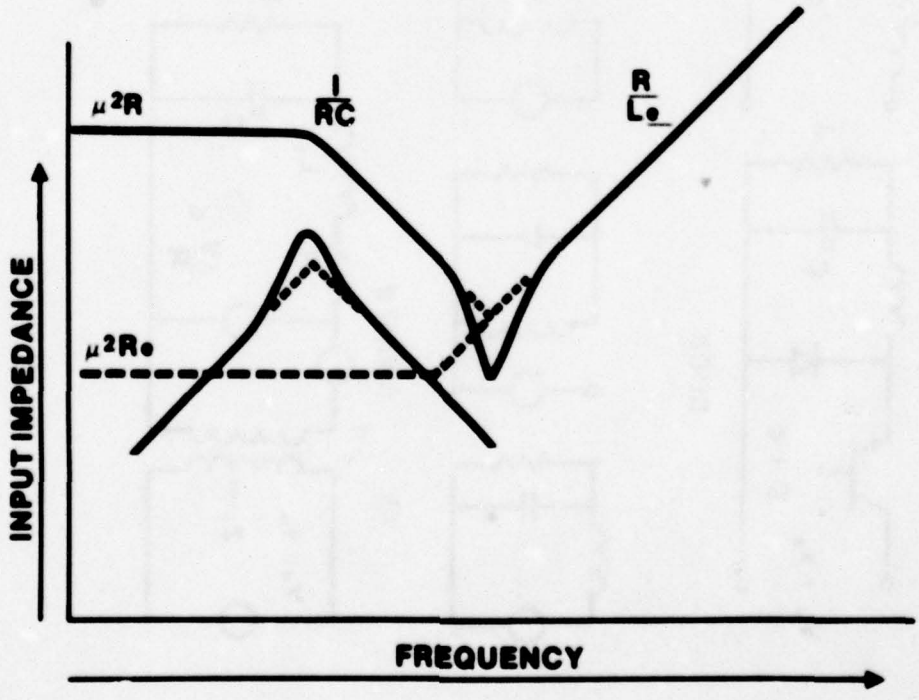

Figure C-4. Middlebrook (1976) stability criteria.

where Z_{ei} is the impedance of the series-resonant averaging filter. Z_i equals $\mu^2 R$ at dc and low frequencies, declines along the asymptote $\mu^2/\omega C$ above $1/RC$, reaches a minimum of $\mu^2 R_e$ at the averaging filter cut-off frequency $\omega_o = 1/\sqrt{L_e C}$, and then rises along the asymptote $\omega\mu^2 L_e$. The upper curve in figure C-4 illustrates $|\mu Z_{ei}|$ (assuming the good approximation $R_e \ll R$). Figure C-4's upper curve also represents the minimum value of $|Z_i|$ at low frequencies because f(s) in general represents a zero and the effect of f(s) is thereby omitted. Note that for stability the Z_s (the lower solid curve in figure C-4) must lie below Z_i at any frequency.

For Z_O to be unaffected a more stringent criterion is required, that

$$|Z_s| \ll |\mu^2(R_e + sL_e)|,$$

where Z_o is the output impedance of the regulator. In figure C-4, $|\mu^2(R_e + sL_e)|$ is represented by the dashed line and to meet this criterion, Z_s must lie below this dashed line.

Graphical techniques demonstrated by Dr. Middlebrook for analyzing one and two section LC input filters will be presented using optimum filters designed by Dr. Yu, et al.

YU, ET AL. (TRW) DESIGN OPTIMIZATION METHODOLOGY

A power processing optimization methodology is presented in reference C2 to meet required specifications for a design and concurrently to optimize a given design quantity. Such a quantity can be weight, efficiency, regulator response, or any other physically-realizable entity. Three inductor design examples are given to demonstrate the methodology:

1. A minimum weight inductor with the wire size predetermined;
2. A minimum weight inductor subject to a given loss constraint; and
3. A minimum loss inductor subject to a given weight constraint.

Computer programs have been prepared by TRW for these optimum inductor designs as part of the Modeling and Analysis of Power Processing Systems (MAPPS) project, sponsored by NASA Lewis Research Center under Contract #NA3-19690.*

Also given in the TRW report are more complex optimum weight designs, one for a single-stage and a second for a two-stage filter. These designs are compared. Theoretical equations and an example are given for each filter. To facilitate a realistic comparison, four requirements were assumed identical for both filters:

F: frequency of switching current = 20 kHz

G: attenuation required at frequency F = 0.002 (-54 dB)

I_{dc}: dc current in inductors = 3 amps

P: power loss allowed = 0.6 watts

---

*NOSC has verified the program's utility by trial applications and is in the process of publishing a report entitled "Optimum Inductor Designs, Theory, Descriptions, Computer Testings, and Validation Results," by E. Kamm. By circulating such reports the intent is to enable power electronics designers to more easily design and improve the performance of their equipment.

Single-Section Optimum Weight Filter

Figure C-5 shows the schematic of the resultant minimum weight one-stage filter (499 grams*). Using techniques described by Middlebrook in reference C1, a graphical analysis is also shown in figure C-5. The graphical analysis enables one to predict the attenuation beyond 20 kHz – the slope is -40 dB per decade (assuming components are frequency invariant). The filter frequency turns out to be

$$f_o = 1/2\pi\sqrt{LC} = 895 \text{ Hz},$$

and its resonant peaking is

$$20 \log Q = 20 \log(\omega_o L/R) = 6 \text{ dB}.$$

Note that the approximate graphical analysis results in almost exactly -54 dB at 20 kHz (the design requirement).

Two-Section Optimum Weight Filter

Figure C-6 shows the schematic of the resultant minimum weight two-stage filter (171 grams**). Here again graphical analysis permits attenuation evaluation at frequencies

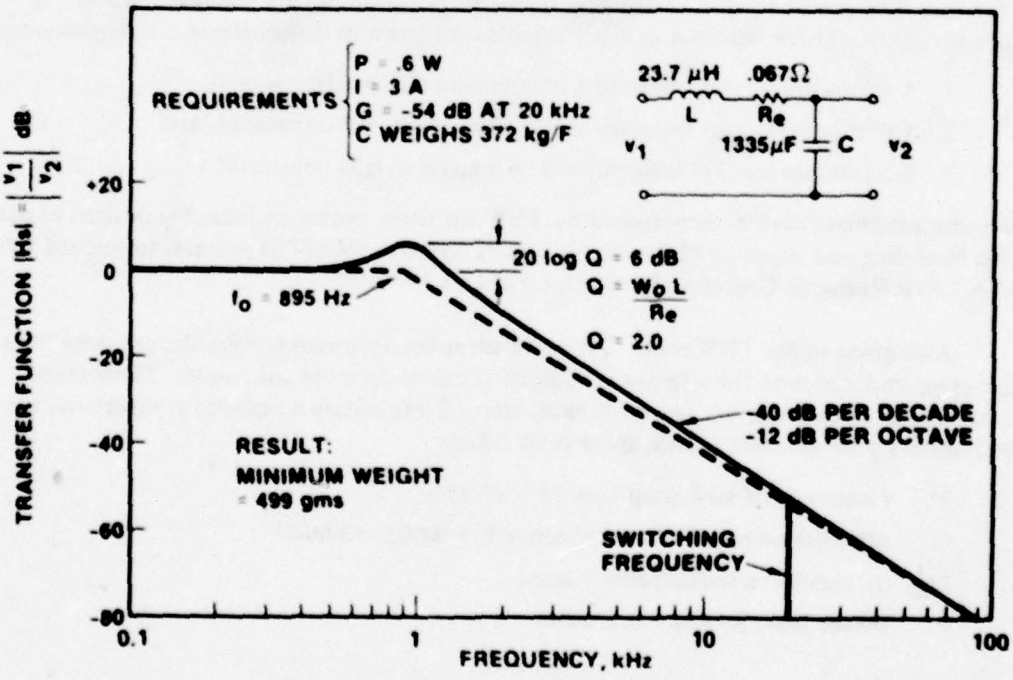

Figure C-5. Single-section optimum weight filter.

*Assumes foil tantalum capacitor, 372 kg/F.

**Assumes foil tantalum capacitor for C_1 (372 kg/F) and poly-carbonate capacitor for C_2 (2600 kg/F).

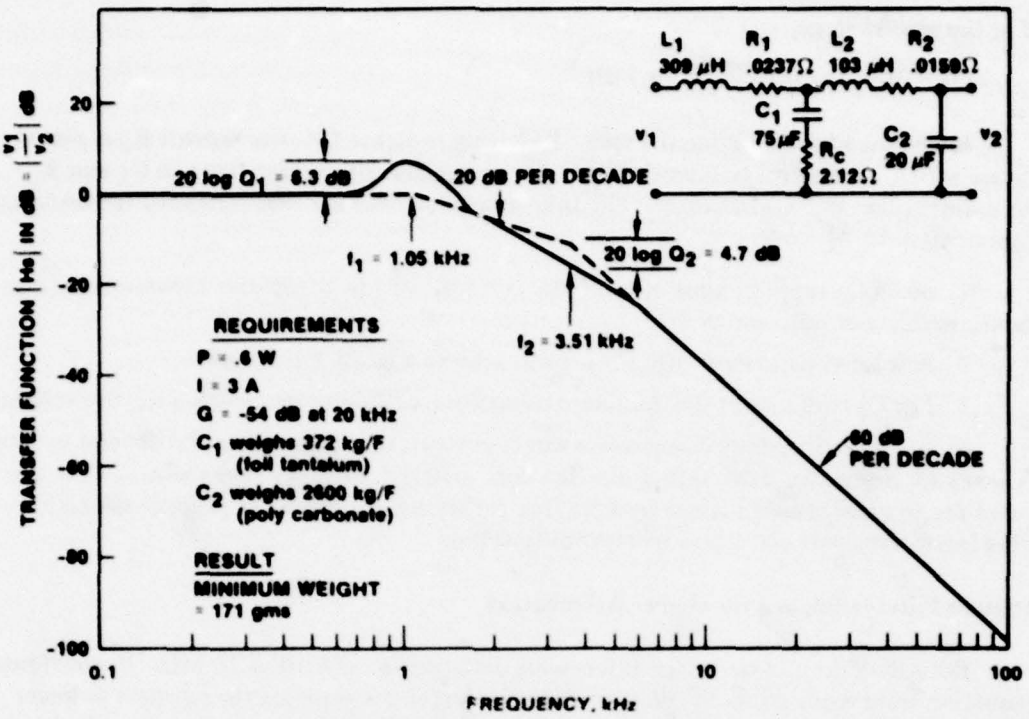

Figure C-6. Two-section optimum weight filter.

other than 20 kHz – the slope is –60 dB per decade beyond 20 kHz (assuming constant parameters). The filter transfer function contains four poles and one zero. At the lower resonant frequency

$$\omega_1^2 = 1/L_1C_1 = 4.3 \times 10^7$$

$$f_1 = \omega_1/2\pi = 1.05 \text{ kHz}.$$

At the higher resonant frequency,

$$\omega_2^2 = 1/L_2C_2 = 4.85 \times 10^8$$

$$f_2 = \omega_2/2\pi = 3.51 \text{ kHz}.$$

Resonant peaking at the first stage filter (Q1) (neglecting the small inductor resistance) calculates to be (reference C2):

$$Q_1 = 20 \log_{10} \sqrt{(1 + L_1/C_1R_c^2)/((C_2/C_1)^2 + (L_1/C_1R_c^2)(1 - C_2/C_1 - L_2C_2/L_1C_1)^2)}.$$

Thus,

$$Q_1 = 20 \log_{10} \sqrt{(1 + (R_1/R_c)^2)/((C_2/C_1)^2 + (R_1/R_c)^2[1 - C_2/C_1 - (\omega_1/\omega_2)^2]^2)}$$

$$Q_1 = 20 \log_{10} 2.05 - 6.3 \text{ dB},$$

and at the second stage,

$$Q_2 = 20 \log_{10} \sqrt{L_2/L_1} = -4.7 \text{ dB}.$$

Recommended Component Types. Referring to figure C-6, the resistor R_c is placed in series with C, to control resonant peaking because negligible current flows in C_1 and R_c except during line and load changes. The following guidelines are recommended for selecting components.[C3,C4,C5,C6]

1. Since C_2 supplies most of the pulse current, use low-dissipative capacitors such as ceramic, mylar, and poly-carbonate.

2. Powdered permalloy core for L_2 will achieve a small core loss.

3. For C_1, foil or wet-slug tantalum capacitors, or aluminum electrolytics are suitable.

4. Inductor L_1 passes essentially a direct current, therefore, eddy current and hysteresis losses are negligible. High saturation flux core material, such as gapped silicon steel, can be used for size and weight savings (reserve flux capability is required to prevent saturation during input transients and audio susceptibility tests).

Optimum Filters Designed for Higher Attenuation

Both the one- and two-stage filters were designed for -54 dB at 20 kHz. If additional attenuation were required, both filters would need larger components (to resonate at lower frequencies). This would be less costly with the two-stage filter since the slope is -60 dB per decade. (For example, another 10.6 dB of attenuation could be obtained by shifting the entire curve in figure C-6 to the left so that f_1 is 700 Hz. Whereas in figure C-5, 10.6 dB additional attenuation would require shifting the resonant frequency to 486 Hz.)

Using the same filters, additional attenuation can be achieved by increasing the switching frequency. For example, if the frequency were doubled to 40 kHz the single-section filter (figure C-1) would increase its attenuation 12 dB at the new switching frequency (from -54 dB to -66 dB). The two-section filter (figure C-2) would increase its attenuation even more (18 dB), resulting in 72 dB at the new switching frequency. Higher switching frequencies would result in even higher attenuations.

CAPACITOR CONSIDERATIONS

Capacitors are neither ideal nor frequency invariant. Typical low ESR/ESL aluminum electrolytic capacitors (reference C4) lose about 15 to 50% capacitance from 120 Hz to 10 kHz and lose 25 to 50% of the remaining capacitance per decade above 10 kHz, settling at

---

[C3] Yu, Y., and Bress, J. J., "Some Design Aspects Concerning Input Filters for DC-DC Converters," paper presented at the IEEE Power Conditioning Specialists Conference, Pasadena, CA, April 1971.

[C4] Macomber, L. L., "Switching Regulator Capacitor Technology: Optimizing Ripple and EMI Suppression Performance," paper presented at POWERCON 5 in San Francisco, CA, 6 May 1978.

[C5] Silber, D., "Simplifying the Switching Regulator Input Filter," Solid State Power Conversion, May/June 1975.

[C6] Cowdell, R. B., "Bypass Filters Extend to the GHz range when Solid-Tantalum Capacitors Are Used," Electronic Design 15, 19 July 1977.

a high frequency value of less than 1% of the 120-Hz capacitance. ESR also decreases with frequency but for low voltage capacitors, increases again. (For example, a 6-V dc capacitor typically decreases with frequency about 40% from 120 Hz to a minimum near 1 MHz. The ESR then typically increases with frequency to within 25% of the 120-Hz value above 10 MHz.) ESL is relatively independent of frequency, but it depends enormously on the capacitor's construction (if designed for fast manufacturability ESL typically runs more than 50 nH but low ESL aluminum electrolytic capacitors run between 0.5 and 15 nH). The net effect is to reduce the capacitor's attenuation ability at high frequencies. Above approximately 150 kHz, the capacitor's ability to attenuate EMI depends almost entirely on ESL. A high voltage capacitor especially designed for low ESL might be expected to provide 2–6 dB additional noise attenuation at 1 MHz and 18 dB at 150 kHz. Experimental results (reference C4) using a 20-kHz power supply drawing 3 amps and a low ESL input capacitor resulted in conducted EMI values of 12 dBμA at 150 kHz, −15 dBμA at 500 kHz, −16 dBμA at 1 MHz, −26 dBμA at 5 MHz, −30 dBμA at 10 MHz, and −26 dBμA at 30 MHz (these points are plotted in figure 15).

ESR and capacitance decrease with increased frequency for those capacitors generally suited to switching regulator input filter applications (aluminum electrolytic, tantalum foil, tantalum wet slug, and solid aluminum, reference C5). For example, it is not uncommon to find the capacitance or ESR of tantalum wet slug capacitors at 50 kHz equal to 50% of their 120-Hz rated values. The lowered capacitance results in a higher ripple voltage across the capacitor in the time domain (at the switching frequency). Referring to figure C-5 for the on-stage filter, the frequency domain curves would be less steep because attenuation, v_2/v_1, at any frequency is inversely proportional to a capacitive function ($v_2/v_1 = 1/(1 + j\omega RC + \omega^2 LC)$). (Note: Silber (reference C5) also recommends a uniformly wound ungapped toroid for the filter inductor if radiated EMI is to be minimized.)

Solid-tantalum capacitors are recommended (reference C6) for bypass filtering because they have low internal inductance and resistance and thus do not resonate until well beyond 1 GHz. They can handle 5 to 100-V dc, and come in a wide range of capacitances. Even so, with an ESL of approximately 20 μH the capacitance decreases with frequency. Cowdell (reference C6) also discusses the effect of lead length: at frequencies below 100 kHz, lead lengths to about 1.5 inches (totaling 3 inches) have little effect on the insertion loss. At higher frequencies, however, lead length increasingly downgrades the insertion loss capability of capacitors (so that the insertion loss may decrease about 12 dB at 1 MHz with a 3-inch total lead length).

LOSSLESS RESONANT DAMPING

It is usually undesirable to have a significant degree of peaking either in the transfer functions (H_e) or the output impedance (Z_s) of the input filter. A high Q transfer function may overload the error amplifier and, for stability, Z_s should be small compared to $\mu^2 Z_{ei}$. (See figure C-4 and page 44.)

In a recent paper, Middlebrook[C7] recommends a circuit for a single-section filter which will achieve resonant damping without decreasing filter efficiency. The damping of a

---

[C7] Middlebrook, R., "Design Techniques for Preventing Input Filter Oscillations in Switched Mode Regulators," paper presented at Power Conference 5, San Francisco, CA, May 1978.

single-section LC filter (figure C-7) is determined by three resistances: two in series (one with inductance (R_e) and one with capacitance R_c), and one in shunt (R) (across the capacitance and its series resistance). Increasing any of the series resistances is undesirable (resulting in less efficiency or introducing a zero in the transfer function). A preferable solution is to parallel the load resistance with a series combination of additional damping shunt resistance and a blocking capacitor (to avoid power loss). This solution is represented in figure C-8. The parasitic series resistances and load resistance are omitted since damping is to be controlled by R_d which defines a Q factor,

$$Q = R_d/R_o$$

where $R_o = \sqrt{L/C}$ is the characteristic resistance of the filter. The blocking capacitor is defined as n times the original filter capacitance C.

An optimum damping resistance R_o exists for a given blocking capacitance value but the optimum R_o (to get optimum Q) is different for the three properties of concern; transfer function (H), input impedance (Z_i) and output impedance (Z_o). If damping of one property is optimized, those of the other two will not be optimized. In applications to switching regulators, therefore, compromises are necessary which nevertheless allow a smaller value of blocking capacitance to be employed than otherwise would be the case.

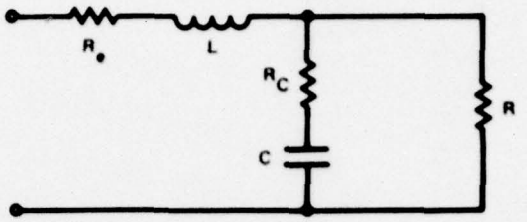

$$Q = \frac{R_o}{R_{te}} \quad \text{DEGREE OF DAMPING AT } \omega_o$$

Where $R_o = \sqrt{\frac{L}{C}}$

$$\omega_o = \frac{1}{\sqrt{LC}}$$

And $R_{te} = R_e + R_c + R_o^2/R$

= TOTAL EFFECTIVE DAMPING RESISTANCE

Figure C-7. Q of an LC filter.

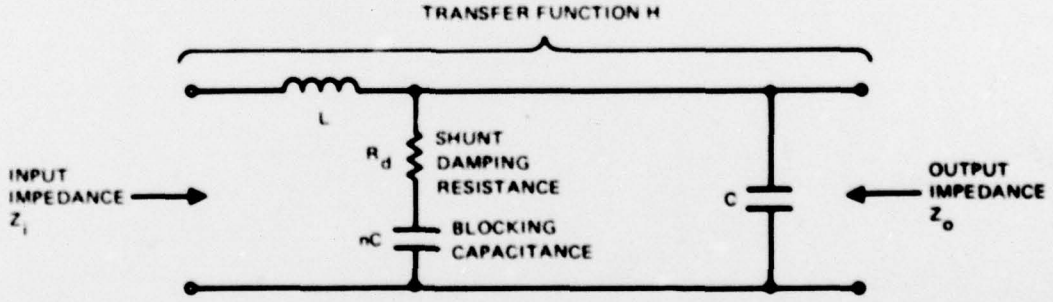

Figure C-8. Single-section low-pass LC filter with blocked shunt damping resistance.

APPENDIX D. RECEIVER SENSITIVITY CONSIDERATIONS

One definition for receiver sensitivity, S, given internal noise power, N, is

$$\frac{S + N}{N} = 2$$

or

$$S = N.$$

For a receiver front end at a typical room temperature (T = 21°C),[D1] the internal noise power expressed in decibels is

$$N(dBm) = -114(dBm) + F(dB) + 10 \log_{10} B(MHz),$$

where F is the noise figure of the receiver and B is the receiver bandwidth in hertz. This definition is in terms of receiver thermal noise which is incoherent and holds for either narrowband signals or broadband incoherent noise. Assuming a 50-ohm system and converting noise power into noise volts:

$$S(dB\mu V) = N(dB\mu V) = N(dBm) + 107(dB)$$

$$= -7(dBm) + F(dB) + 10 \log_{10} B(MHz).$$

For the 20-kHz region where the calculations are being done, a receiver noise figure (F) of 2 dB was used which is valid now and expected to be valid in the future. A narrowband calculation was performed because the receiver sensitivities are narrower than the switching frequency harmonics spectrum interval (only one harmonic would be received at each receiver setting). The most sensitive receiver has the narrowest bandwidth. In this case, it is a receiver with a bandwidth of 200 Hz and the sensitivity calculates to be

$$S(dB\mu V) = -7 + 2 + 10 \log (10^6/200) = -42(dB\mu V).$$

This sensitivity information was further confirmed by discussions with personnel at NUSC who gave a lower limit of 6 nV for sensitivity (6 nV corresponds to -44 dBμV).

[D1] White, D. R., Electromagnetic Interference and Compatibility, Vol 2 pgs 3.68-3.71, Don White Consultants, Inc., 1976.

APPENDIX E. CALCULATIONS TO DETERMINE SEPARATION DISTANCES TO PRECLUDE INTERFERENCE

MAXIMUM PERMITTED FLUX DENSITIES

To limit the voltages induced into the receiver cables requires limiting the magnetic field. However, the limiting value of magnetic flux density will depend upon the cable characteristics. (See page 19 in main text.)

For the less susceptible receiving cable of 11 dBμV/μT, the flux density (B) limit at 20 kHz required to limit the induced voltages to -64 dBμV (includes the 20-dB safety factor) is

*B(dBμT) = -64 dBμV - (11 dBμV/μT)

= -75 dBμT for 2 SWF cable at 20 kHz.

For the more susceptible cables of 34 dBμV/μT, the flux density (B) limit at 20 kHz required to limit the induced voltage to -64 dBμV, including 20-dB safety factor, is

B(dBμT) = -64 dBμV - 34 dBμV/μT

= -98 dBμT for RG-264A/U cable at 20 kHz.

POWERLINE-GENERATED FLUX DENSITIES

The magnetic flux density surrounding the powerline cable depends upon the physical characteristics and dimensions of the powerline, the current, and the distance from the cable. (For more information, see main text section, "Magnetic Field Emissions.") The tables prepared by NUSC (reference 13) were used to determine the distances required to achieve the above limiting flux densities. These distances were found for three sizes of the TSGU type cable (the DSGU types have identical distances) and also for different amplitudes of line current. The NUSC tables tabulate flux densities in dBμT at intervals of one inch for cables carrying one ampere of current. As shown in figure 15, for a one-ampere pulse, the predicted noise current at 20 kHz (using the two-section filter) would be 60 dB down from one ampere (-60 dBA). Correspondingly, a 10-ampere pulse would generate -40 dBA at 20 kHz and 100 amperes would result in a -20 dBA component at 20 kHz. Tables E-1 through E-3 list the flux densities for required current values at one-inch increments from the cables.

NOTE: Calculations were only performed at 20 kHz, the frequency at which the maximum induced voltage would occur. This is true because the induced voltage is linearly proportional to both the magnetic field and frequency, at a given distance. The magnetic field frequency component (proportional to the current component) decreases more rapidly than 20 dB per decade with increasing frequency up to 1 MHz (figure 15); and correspondingly

---

*From main text,
V/B(dB) = 11 dBμV/μT
therefore V(dBμV) - B(dBμT) = 11 dBμV/μT
so for VdBμV = -64 dBμV
B(dBμT) = -64 dBμV - (11 dBμV/μT)

affects the induced voltage. Increasing the frequency causes an increasing 20-dB-per-decade change in the induced voltage. The net result is a decrease in induced voltage up to 1 MHz, and beyond 1 MHz much less sensitivity is required (figure 17).

Table E-1. Magnetic flux density versus distance from cable for types TSGU-3 and DSGU-3 cables (maximum current is 12.0 A).

Distance from Cable, inch	Flux Density, dB microtelsa		
	1-amp Cable Current	-60 dBA Cable Current (filtered 1 amp)	-40 dBA Cable Current (filtered 10 amp)
0	48.38	-11.62	8.38
1	0.17	-59.83	-39.83
2	-26.85	-86.85*	-66.85
3	-46.22	-106.22**	-86.22*
4	-65.07	-125.07	-105.07**

*Maximum acceptable flux densities ≤ -75 dBμT.
**Maximum acceptable flux densities ≤ -98 dBμT.

Table E-2. Magnetic flux density versus distance from cable for types TSGU-100 and DSGU-100 cables (maximum current is 183.0 amps).

Distance from Cable, inch	Flux Density, dB microtelsa			
	1-amp Cable Current	-60 dBA Cable Current (filtered 1 amp)	-40 dBA Cable Current (filtered 10 A)	-20 dBA Cable Current (filtered 100 A)
3	-8.07	-68.07		
4	-20.20	-80.20*		
5	-26.18	-86.18	-66.18	
6	-31.97	-91.97	-71.97	
7	-37.65	-97.65**	-77.65*	
8	-43.24		-83.24	
9	-48.76		-88.76	-68.76
10	-54.22		-94.22	-74.22
11	-59.64		-99.64**	-79.64*
12	-65.03			-85.03
13	-70.38			-90.38
14	-75.71			-95.71
15	-81.02			-101.02**

*Maximum acceptable flux densities ≤ -75 dBμT.
**Maximum acceptable flux densities ≤ -98 dBμT.

Table E-3. Magnetic flux density versus distance from cable for types TSGU-200 and DSGU-200 cables (maximum current is 284.0 amps).

Distance from Cable, inch	Flux Density, dB microtelsa				
	1-amp Cable Current	-60 dBA Cable Current (filtered 1 amp)	-40 dBA Cable Current (filtered 10 A)	-20 dBA Cable Current (filtered 100 A)	-14 dBA Cable Current (filtered 200 A)
5	-14.03	-74.03	-54.03		
6	-24.91	-84.91*	-64.91		
8	-33.34	-93.34	-73.34		
9	-37.44	-97.44	-77.44		
10	-41.49	-101.49**	-81.49*		
14	-57.31		-97.31	-77.31	-71.31
15	-61.20		-101.20**	-81.20*	-75.20
16	-65.07			-85.07	-79.07*
17	-68.93			-88.93	-82.93
19	-76.59			-96.59	-90.59
20	-80.40			-100.40**	-94.40
21	-84.20				-98.20**

*Maximum acceptable flux densities ≤ 75 dBμT.
**Maximum acceptable flux densities ≤ -98 dBμT.

APPENDIX F. EMI SUPPRESSION TECHNIQUES FOR SWITCHING-MODE POWER SUPPLIES

INTRODUCTION

Techniques are discussed here to reduce EMI caused by the steep rise and fall of the switching waveform. The EMI suppression methods include using fast (but soft) recovery diodes, controlling the shape of transistor rise and fall times, using low EMI wiring techniques and possibly shielding, filtering input and output leads, and EMI confinement techniques for transformers and inductors.

Use of Fast (Soft) Recovery Diodes

Diodes are nonideal and exhibit a phenomenon known as reverse recovery. A spike occurs at the end of a diode conduction cycle when reverse voltage is applied by the transistor. A short pulse of reverse current through the diode is required to sweep out minority carriers and to establish the reverse biased junction. The transistor must supply this current in addition to the commutated inductor current. Therefore, there is a corresponding transistor current spike. This effect can be limited by the use of a fast recovery diode.

Where the Schottky diode (reference 21) is applicable, one can obtain virtual freedom from this source of noise. Schottky diodes have low forward voltage drops but their reverse leakage current increases with high reverse voltages. At the present time, low reverse current Schottky rectifiers are obtainable[F1,F2] with acceptably low reverse current and reverse voltage capabilities up to 45 or 50 volts. A safety factor is recommended, however, limiting their use to lower voltages. For higher voltages, other types of fast recovery diodes become increasingly competitive as forward voltage drop diminishes in importance. Blatt (reference F1) gives peak recovery current data at 25° and 125°C for various fast recovery diodes (including the Schottky). For a 30-amp forward current (with di/dt = 30 A/μsec), the maximum recovery current (at 125°C) was 1.0 amp for the Schottky, 3.7 amps for a 100-nsec rectifier.

These fast recovery diodes, however, can generate radiated energy due to the steep di/dt. To control this radiation, use ferrite beads on transformer output leads feeding rectifier diodes and capacitors across the diodes.[F3] New high speed rectifiers are now available which have a soft recovery characteristic; reducing the di/dt on turn-off and reducing the need for beads and capacitors.

Control of Transistor Rise and Fall Times

Fast rise/fall time transistors result in more efficient switching-mode power supplies. Unless controlled, they also result in high frequency radiated emissions.

[F1] Blatt, F. M., "Pick the Right 'fast' Rectifiers to Design Switchers Effectively," EDN, 20 January 1978.

[F2] Roehr, B., "Transient Response Measurements of High Speed Rectifier Diodes," a Motorola Semiconductor Group paper.

[F3] Bloom, S. D., and Massey, R. P. (Bell Laboratories), "Emission Standards and Design Techniques for EMI Control of Multiple DC-DC Converter Systems," paper presented at IEEE Power Electronics Specialists Conference, Cleveland, Ohio, 10 June 1976.

Bloom and Massey (reference F3) soften their main switching waveforms by controlling the base drive of the main power switching transistors. The turn-on time of the transistor is limited by the inductance of their power transformer, while the turn-off time is slowed down to one microsecond by a signal derived from an RC network across the transformer. The RC network also absorbs the inductive energy stored in the transformer.

Two basic snubbing configurations are shown in figure F-1. Design equations for six types of switching regulator and regulator/converter circuits are given in reference F4. For the current snubber, most of the power dissipated in the snubber would otherwise be dissipated in or radiated from the transistor. The voltage snubber can lead indirectly to improved efficiency by allowing for a lower average junction temperature. Recommendations are also made for component selection for the passive elements of the two snubbers considering the transient performance in addition to the normal voltage, current and power constraints. They state that more elegant techniques are available to those who are willing to trade simplicity for greater efficiency.

At high power levels Calkin and Hamilton[F5,F6] remove most of the switching losses from the switching transistor with two networks, each containing three components: an inductor or a capacitor, a diode, and a resistor. With proper design they even somewhat improve the overall efficiency.

Mechanical Suppression Techniques and High Frequency Filtering

To minimize internal radiation, all switched current leads should be kept short and the hot and return leads twisted, or where the wiring is a printed circuit the hot and return leads should be run in mirror-image conductors. This also applies to parts of the circuit that carry low switched currents because in a high impedance circuit significant radiation can still occur (reference F3). Gottlieb (reference 21) recommends that the grounding of the large input capacitor, together with that of the diode, be made separate from all other components. Care should be exerted to avoid inductive loops wherever possible. Also, the wiring layout should aim for capacitive isolation of high dV/dt point in the circuit.

It will usually be necessary to enclose the power supply in an attenuating enclosure. Considerable shielding information is contained in a recent book by Ott (reference 22) which also covers detailed noise suppression information in general. For shielded enclosures to be effective, all leads entering or leaving the shield should be filtered to prevent them from conducting noise out of the shield. In some cases (for lower frequencies), normal decoupling filters are adequate. At higher frequencies, however, special care must be taken to guarantee the effectiveness of the filter. Ott recommends the use of feedthrough capacitors where the conductor passes through the shield; and a mica or ceramic capacitor, with short leads,

---

[F4] Skanadore, W. R., "Methods for Utilizing High Speed Switching Transistors in High Energy Switching Environments," publication from General Semiconductor Industries, Inc., P. O. Box 3078, Tempe, Arizona 85281, December 1977.

[F5] Calkin, E. T. and Hamilton, B. H., "Circuit Techniques for Improving the Switching Loci of Transistor Switches in Switching Regulators," IEEE Transactions on Industry Applications, Vol. IA-12, July-August 1976.

[F6] Calkin, E. T., and Hamilton, B. H., "A Conceptually New Approach for Regulated DC to DC Converters Employing Transistor Switches and Pulsewidth Control," IEEE Transactions on Industry Applications, Vol. IA-12, July-August, 1976.

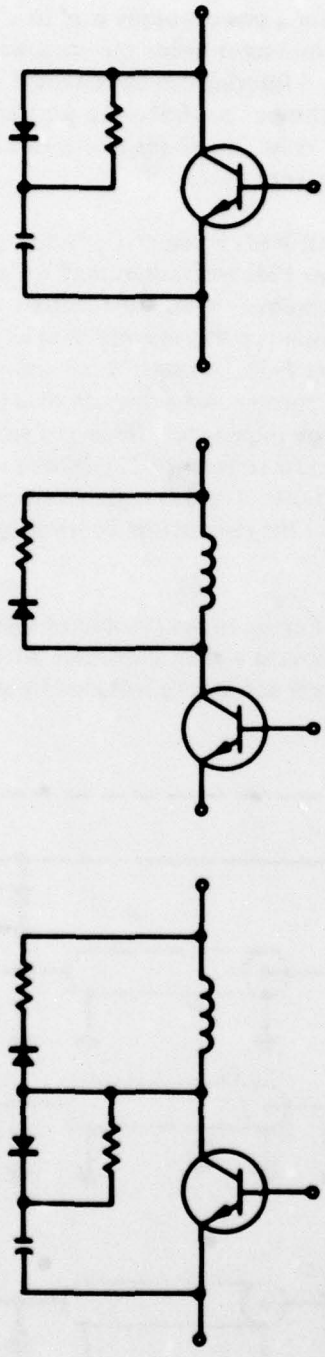

a) TURN-OFF (CURRENT) SNUBBER

b) TURN-ON (VOLTAGE) SNUBBER

c) IMPLEMENTATION OF VOLTAGE AND CURRENT SNUBBER

Figure F-1. Voltage and current snubbers.

between the conductor and ground at the circuit end. (NOTE: Feed-through capacitors have very low self-inductance [no lead length] and, therefore, have better performance at higher frequencies.) Three other ways to filter a power supply lead to a high frequency circuit are shown in figure F-2. Shielding the conductor inside the enclosure decreases the noise picked up by the conductor. Additional filtering can be obtained with a C-L-C pi-filter. This pi-filter can be further improved by enclosing the choke in a separate shield, inside the primary shield to prevent it from picking up noise. In all the above filters, the lead lengths on the capacitors and shield grounds must be kept short.

Although filtering of input and output leads is essential, packaging in a shielded enclosure may not always be necessary. Use of low EMI techniques may be sufficient to permit open-frame power supplies. Some newer techniques being used include the use of lossy ferrites in balun and other line inductors. A balun is a transformer used as a longitudinal choke (also called a neutralizing transformer) (figure F-3). A transformer connected in this manner presents a low impedance to the differential current and allows dc coupling. To any common-mode noise, however, the transformer is a high impedance. Thus the ground loop is broken without the use of an isolating transformer. Ott (reference 22) develops circuit equations for both the differential and common-mode currents. He also suggests an easy way to place a longitudinal choke in the circuit; simply wind the conductors connecting the two circuits around a magnetic core as shown in figure F-4.

Another use for ferrites is as beads. Ferrite beads provide an inexpensive and convenient way to add high frequency resistive loss in a circuit without introducing power loss at dc and low frequencies. The beads are small and can be installed by slipping them over a

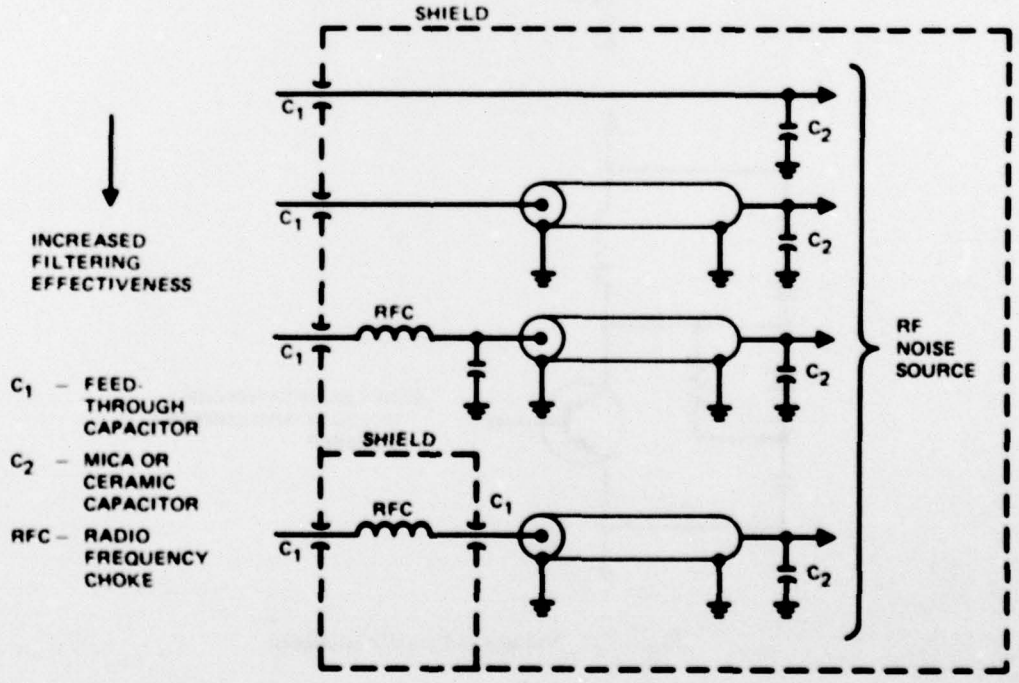

Figure F-2. Four high frequency lead filtering methods.

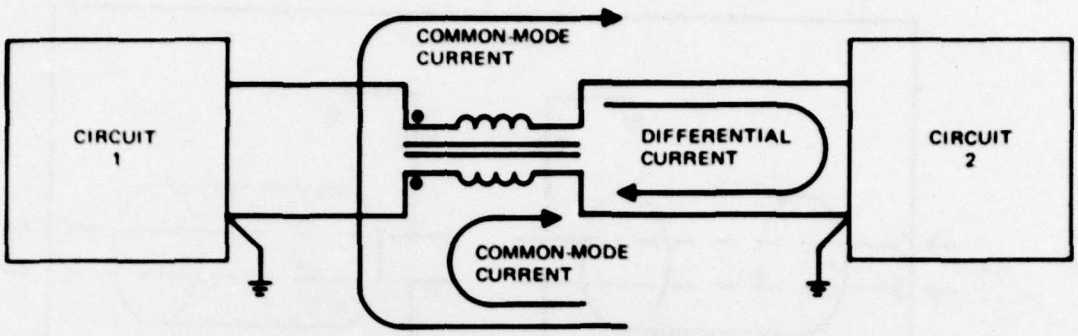

Figure F-3. Balun or neutralizing transformer.

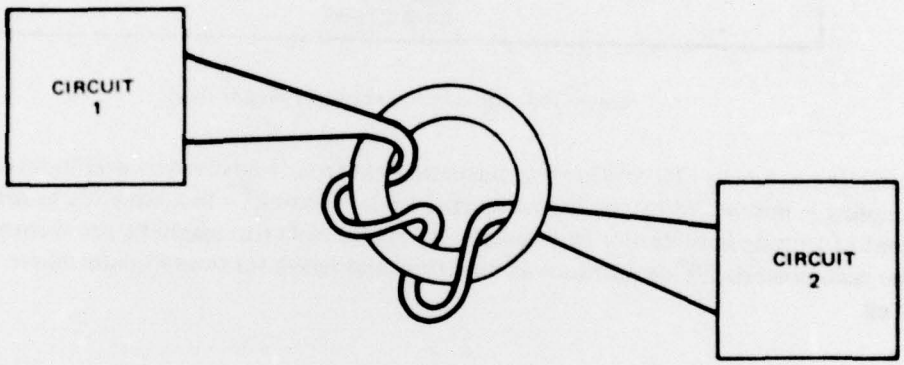

Figure F-4. An easy way to wind a balun.

component lead or conductor. They are most effective above 1 MHz and can provide high frequency decoupling, parasitic suppression and shielding. They are being used to damp out the high frequency oscillations generated by switching transients. If a single bead does not provide sufficient attenuation, two or three beads may be used. They are frequently used as part of an EMI LC filter. To reduce common-mode conducted emission, Bloom and Massey (reference F3) place a mylar capacitor from each input and output lead to ground and route the input and output leads through ferrite beads (figure F-5). The relatively lossy mylar dielectrics (compared to conventional ceramic or mica dielectrics) help dissipate the high frequency energy.

EMI Confinement Techniques for Transformers and Inductors

Transformers, not being ideal, have capacitance between primary and secondary windings, and this allows noise coupling through the transformer. This coupling can be reduced by providing a properly grounded electrostatic, or Farraday, shield (a grounded conductor between the two windings). Inductors wound on closed magnetic cores have less external magnetic field than open cores. If necessary, high-permeability magnetic shielding

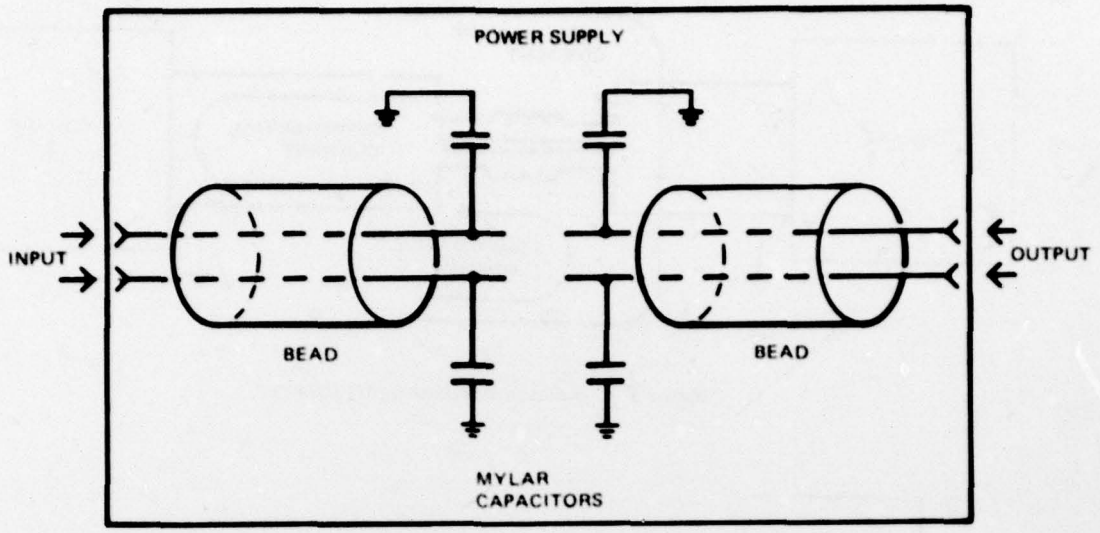

Figure F-5. Input/output bead, capacitor filter.

material can be used to confine the magnetic field from transformers and inductors. Magnetic coupling is minimized by the use of twisted leads. Hnatek[F7] recommends quadrature placement of toroids in reference to adjacent toroids to minimize magnetic cross-coupling. He also recommends 90° orientation of high-level and low-level twisted pairs where they must cross.

[F7] Hnatek, E. R., Design of Solid-State Power Supplies, Van Nostrand Reinhold Co., 1971.